第 III-2 章　第2年次調査への提言

1991～1994 年度に実施されたブグニ地域での地質・地化学調査の結果，Kékoro 地域において強い Au 地化学異常と同時に，多数の鉱徴地が存在することが報告された。これを受けた今回(1997 年度)のケコロ・バオレ－バニフィング地域第1年次調査では，地化学探査，鉱徴地調査，衛星画像解析等を実施した。

地化学探査では Kékoro 地域から北西方向に伸びる3列の明瞭な Au 地化学異常を見いだした。

鉱徴地調査では新たな鉱徴地を発見したほか，ラテライト性皮殻中の多数のピット群からなる鉱徴地は，砂鉱床ではなく，初生金鉱床がラテライト性風化作用によって金が風化断面中の複数の層準に移動・富化したものであると考えた。すなわち，現在我々は旧ピット群ではラテライト断面中の金が富化した表層部をみているものと判断した。

今回の調査結果から得られた地質・地化学的証拠をまとめ，地下深部に期待される鉱床探査の優先順位を Tableau III-2-1 にまとめた。結論として，最優先すべきと判断されるのは西部 Kékoro 地域の中北部(Kékoro A,B,C)で，ついで Kékoro 地域北部(Kékoro F)，さらに Kékoro 南部(Kékoro D,E)，Sagala，Diamou South が挙げられる。

ラテライト断面中の Au 富化帯およびその初生鉱化帯を探査するためには，風化帯の発達深度を確認し，サプロライト中での Au 富化現象を確認することが必須である。第2年次調査では深部地化学探査が最も有効であろう。

西部 Kékoro 地域中北部を最優先とした第2年次の探査手法を以下にまとめる。

・ベ－スライン，ピケットラインからなる測線設定

・測線上での精密地化学探査および地質調査

・ピット掘削(深度 5-7 m)によるラテライト性皮殻からサプロライト帯上部の地質・地化学調査

・パ－カッションドリル(深度 100 m)による多元素深部地化学探査

・空中写真判読を伴う精密地質図の作成

第2年次の深部地化学探査においてサプロライト中での Au 富化現象が確認された後，第3年次以降にはコア採取を目的とした試錐および鉱化帯の物理探査に移行し，鉱床の評価の段階となるであろう。

Tableau III-2-1 Proposition pour l'étude à venir dans la régions de Kékoro et Banifing-Baoulé

Regional name	Baoulé-Banifing East					Kékoro West			Geochemical anomalous area					
Area name	Soba	Banifing-Baoulé	Kouloukoro	Siriba Sobala	Diamou	Kékoro A,B,C	Kékoro D,E	Kékoro F	Sagala	Diamou South	Torokoro East	Kalako	Sirikoro	Kékoro East
Mining operation	non	pits	pits	pits	pits and trench	pits	pits	pits	non	non	non	non	non	non
Geology	metasediments, diorite, dolerite, laterite, quartz floats	laterite	metasediments, quartz floats	metasediments, quartz floats	metasediments, dacite intrusion, quartz floats	basement floats(pelitic and psamitic shcist, tourmaline sandstone, quartzite, mica schist, biotite granite, granodiorite) granite porphyry, rhyolite intrusion, dolerite, thick laterite, quartz floats			laterite crust, saprolite?	laterite crust, saprolite?	laterite crust, saprolite?	laterite crust, saprolite?	laterite crust, saprolite?	laterite crust
Geological and Geochemical circumstances	on anticlinal axis	geological situation unknown, isolated from Geochemical anomaly zone	along NW-SE lineament		NW-SE lineaments	NS lineaments, strong Geochemical anomaly	NS silicified rhyolite intrusion	porphyritic intrusion?	near boundary from syntechtonic granite, extension of NW-SE lineament from Kékoro	NW-SE lineaments	Distribute along the NW-SE lineaments			Northwest from Donba prospect area
Gold occurrence	hematite quartz vein	laterite (carapace)	laterite (carapace) and quartz vein	laterite (carapace)	sheared zone in Birrimien	laterite (carapace)	laterite(carapace) and rhyolite	laterite(carapace and saprolite)	unknown	unknown	unknown	unknown	unknown	unknown
Direction of Mineralization	N10-20E, 30-70E	massive	WNW-ESE	WNW-ESE	WNW-ESE, NNE-SSW	NS	NS	massive?	unknown	unknown	unknown	unknown	unknown	unknown
Dimension of mineralized area	area of floats 400 m x 200 m	300 m*150 m	300 m	<500 m	130 m*40 m	A: NE-SW1000m*70m, NS600m*100m, B: NS600m*250m, EW900m*200m, C: EW,1700m*150m	D: 550m*150m, 200m*80m, 400m*150m, E: 500m*20m	400m*250m	unknown	unknown	unknown	unknown	unknown	unknown
Au ore grade (g/t)	0.01-<0.005 g/t in quartz	1.2 g/t in carapace	0.015-0.005 g/t in qtz and 0.015-0.01 g/t in laterite	unknown	0.89 g/t in sheared zone	A: 0.5-86 g/t(qtz floats), 0.1-0.3 g/t(laterite), B: 0.4 g/t(qtz float)	E: 0.2 g/t(silicified rhyolite)	0.4 g/t (carapace?), 2.7 g/t (saprolite)	no data	no data	no data	no data	no data	no data
Alteration	silicification in dacite, toumaline qtz	unknown	toumaline quartz	unknown	sericite, chlorite, epidote, pyrite	unknown	silicification in rhyolite	unknown	unknown	unknown	unknown	unknown	unknown	unknown
Au Geochemical anomaly	non	non	weak	weak	weak	strong(1,200 ppb max.) to medium	weak to medium	no data	605 ppb(max)	410 ppb(max)	385 ppb(max)	240 ppb(max)	720 ppb(max)	95 ppb(max)
Thickness of laterite profile	thin or no laterite	thick	thin	thin	no laterite	thick	thick	thick	thick	thick	thick	thick	thick	thick
Area of future survey	-	500m*1000m	17 km		300 m*100 m	20 km*12 km		2 km*2 km	4 km*6 km	2 km*4 km	1 km*2 km	2 km*2 km	5 km*3 km	2 km*6 km
Method of future survey	-	pit survey, deep Geochemical survey	geological, Geochemical survey		detailed geological survey	air photo interpretation, detailed geological and Geochemical survey, pit survey, deep Geochemical survey			geological survey and pit survey	geological survey and pit survey	geological survey and pit survey	geological survey and pit survey	geological survey and pit survey	geological survey and pit survey
Rank of priority	-	B	D		C	A	B	A-B	B	B	C	C	B-C	B-C

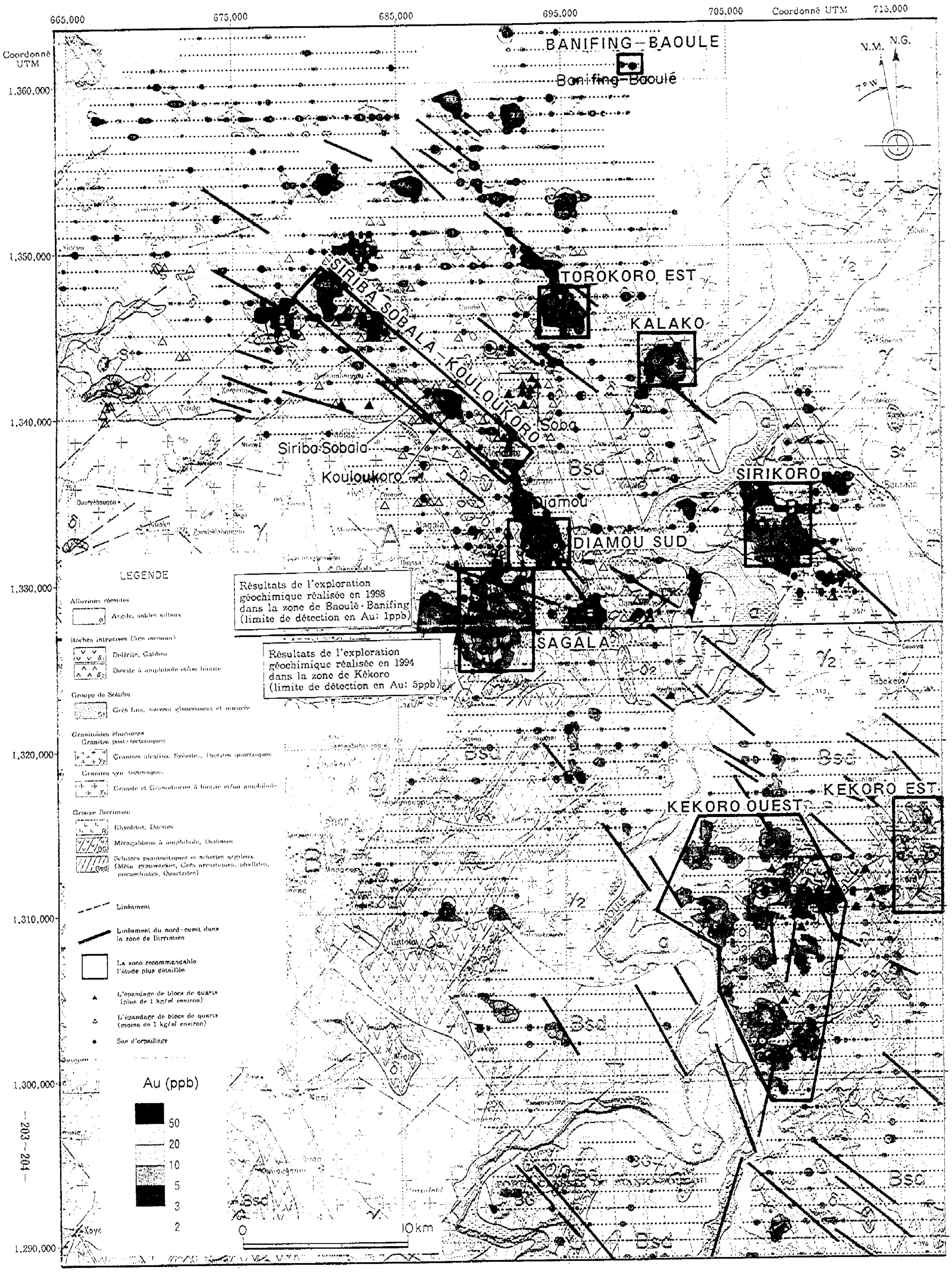

Fig. III-2-1 Proposition pour l'étude à venir dans les régions de Kékoro et Baoulé-Banifing

参考文献

Barros de Oliveira, S. M., Trescases, J. J and José Melfi, A. (1992), Lateritic nickel deposits of Brazil : Mineralium Deposita, v. 27, p. 137-146.

Bassot J. P. et, al (1980). Carte géologique du Mali à 1/1 500000. Ministére du Développment industrial. Direct. Nat. Min., Mali.

Bassot J. P. et, al (1980). Le gisement d'or de Kalana (République du Mali). Chron. Rech. Min., Fr., n457, pp. 5-18

Bassot J. P. et, al (1981). Notice explicative de la carte géologique à 1/1 500000 de la République du Mali. BRGM-DNGM Mali.

Bowell R.J., Afleh E.O., Laffoley N.d'A., Hanssen E., Abe S., Yao R.K., and Pohl D.(1996) : Geochemical exploration for gold in tropical soils-four contrasting case studies from West Africa. Transaction; Institute of mining and metallurgy, section B, Applied Earth Sciences.

Bridges E. M.(1978) : World soils,pp.128, Cambridge University Press.

Butt, C. R. M. (1988). Genesis of Supergene Gold Deposits in the Lateritic Regolith of the Yilgarn Block, Western Australia. Eco. Geo. Mon6.,p460

Colin F. Viellard P. and Ambrossi J.P. (1993): Quantitative approach to physical and chemical gold mobility in equatorial rainforest lateritic environment. Erth Planet. Sci. Lett,. 114,269-85.

DICKO M. T. (1977). Prospection préliminaire de la croute d'altération du gisement d'or de Kalana (Mali). Mém. Fin d'études ENI, Bamako, Mali.

Dahanayake, K. (1982), Laterites of Sri Lanka-A Reconnaissance Study : Mineralium Deposita, v. 17, p. 245-256.

Davies, T. C. and Bloxam, T. W. (1979). Heavy Metal Distribution in Laterites, Southwest of Regent, Freetown Igneous Complex, Sierra Leone. Eco. Geo, vol74, num3, 638p.

Diallo M. (1979). Caractéristiques géochimiques et conditions de concentration de l'or ; cas du gisement de Kalana (Mali). Thése doct. (Ph. D.), URSS.

Diallo M., et, al (1989). Tectonique transcurrente et évolution polycyclique dans le Birrimien, Protérozoique inférieur, du Sénégal-Mali (Afrique de l'Ouest). C. R. Acad. Sci. Fr., 308, sér. II, pp. 117-122

Dommanget A et, al(1985). Un nouvean type de gisement d'or : Loulo (Mali). Chron. Rech. min., Fr., n481, pp.5-18 Translsted into English in a spetial issue of the Chron. Rech. min., Fr. (Jury, 1989).

Dommanget A et, al(1987). Compte rendu de mission en Cote-d'Ivoire et au Mali. Note BRGN/DEX, Fr, n1336

Dommanget A et, al(1989). Découverte d'un gisement d'or encaissé dans des turbidites tourmalinisées, (Mali). (A paraitre)

Dommanget A et, al(1986). Le gisement de Loulo (Mali) : un exemple de concentration aurifére stratiforme dans des grés à tourmaline du Birrimien de l'Afrique de l'Ouest. CIFEG, publication occasionnelle, n10, pp. 123-130

Dommanget, A., Milési, J. P., and Diallo, M., (1993), The Loulo gold and tourmaline-bearing deposit ; a polymorph type in the Early proterozoic of Mali(West Africa) : Mineralium Deposita, v. 28, p. 253-263.

Dostal, J. and Dupuy, C. (1987). Gold in Late Proterozoic Andesites from Northwest Africa. Eco. Geo, vol82, num3, 762p

Duchaufour Ph. (1984): Abreges de Pedologie, Masson, (Nagatsuka S., Japanese edition, Hakueisya 1988)

Eisenlohr, B. N. (1992), Conflicting evidence on the timing of mesothermal and paleoplacer gold mineralisation in early Proterozoic rocks from southwest Ghana, West Africa : Mineralium Deposita, v. 27, p. 23-29

Frakes L. A. : Climate through geologic time(Amsterdame: Elsevier), 1979, 310 p.

Funk and Wagnalls Corp. (1993-1995): "Mali, Republic of", in Microsoft(R) Encarta 1996 [CD-ROM]

Gardner L. R.(1970) : American Mineralogist. Vol.55, p1380.

Hatta Tamao(1994) : Simulation of Mass Transfer on Weathering Process. Journal of Clay Science Society of Japan, Vol.34, pp.165-174.(in Japanese)

Huot, D. Sattran, V. and Zida, P. (1987). Gold in Birrimian Greenstorn Belts of Burkina Faso, West Africa. Eco. Geo, vol82, num8, p2033.

JICA/MMAJ(1992-1994):国際協力事業団・金属鉱業事業団(平成4～6年):マリ共和国ブグニ地域資源開発協力基礎調査報告書

Lajoinie J.P.,Fonteille M.(1968).-Un gite de skarns latérisés : le gite aurifére d'Ity (Côte-d'Ivoire). Chron mines d'outre-mer, n 378, pp. 143-153.

Lajoinie J.P.,Grassaud J.(1962).-Un exemple de gisement d'or latéritique : Ity(Côte-d'Ivoire). Rap. BRGM Inédit, 8p.

Ledru P. et, al (1987). The Proterozoic Linguekoto fan delta, Sénégal-Mali : its occurrence, development and regional implications. Oral comm., cong. « Fan Delta and Tectonic setting », Norvége.

Mann, A. W. (1984), Mobility of Gold and Silver in Lateritic Weathering Profiles : Some Observations from Western Australia. Eco. Geo., vol79, num1, p38

Marcoux, E and Milesi, J. P. (1993). Lead Isotope Signature of Early Proterozoic Ore Deposita in Western Africa : Comparison with Gold Deposits in French Guiana. Eco. Geo., vol88, num7, p1862

Michailidis, K. M. (1990), Zoned chromites with high Mn-contents in the Fe-Ni-Cr-laterite ore deposits from the Edessa area in Northern Greece : Mineralium Deposita, v. 25, p. 190-197

Michel, D., (1987), Concentration of gold in in situ laterites from Mato Grosso : Mineralium Deposita, v. 22, p. 185-189

Milesi J. P. et, al (1989). Diversity of magmatic and tectonic setting in lower Proterozoic of West Africa (Senegal-Mali boundary) : Low-K tholeiites and calcalkalines suites. Abstracts, 28th Int. Geol. Cong., Washington, USA, Jury 9-19, 2-3, p. 434

Milesi J. P. et, al (1989). Lower Proterozoic succession in Senegal and Mali (West Africa) : Position of sediment-hosted Au and Fe deposits of Loulo area and significance in terms of crustal evolution. Abstracts, 28th Int. Geol. Cong., Washington, USA, Jury 9-19, 2-3, pp. 433-434

Milési, J. P., Ledru, P., johan, V., Marcoux, E., and Vinghon, Ch., (1991) : The metallogenic relationship between Birimian and Tarkwaian gold deposita in Ghana : Mineralium Deposita, v. 26, p. 228-237

Mohr E. C. J., van Baren F. A. and van Schuylenborgh J.(1989) : Mali gold jv. Mining Magazine, 160, n 4, p. 257

Mumin, A. H., Fleet, M. E., and Chryssoulis, S. L. (1994) : Gold mineralization in As-rich mesothermal gold ores of the Bogosu-Prestea mining district of the Ashanti Gold Belt, Ghana : remobilization of "invisible"gold : Mineralium Deposita, v. 29, p. 445-460.

Nahon, D., Paquet, H. and Delvigne, J.(1982) :Lateritic Weathering of Ultramafic Rocks and the Concentration of Nickel in the Western Ivory Coast. Eco. Geo, vol77, num5, 1159p.

Olson, S. F. et,al (1992) : Resional Setting, Structure, and Descriptive Geology of the Middle Proterozoic Syama Gold Deposit, Mali, West Africa. Eco. Geo., vol87, num2, p310

Olson, S.F. et al. (1992) : Regional Setting, Structure, and Descriptive Geology of the Middle Proterozoic Syama Gold Deposit, Mali, West Africa

Paul J.Golightly(1981): Nickeliferous Laterite Deposts, Economic Geology, 75th Anniversary Volume,pp.710-735.

Permingeat F., et, al (1970) : Carte des gites minéraux de la République du Mali à 1/10,000,000, inédite.

Republic of Mali / United Nations (1987) : Mineral Resources of MALI

Schellmann, W. (1989) : Composition and origin of lateritic nickl ore at Tagaung Taung, Burma : Mineralium Deposita, v. 24, p. 161-168

Soil Survey Staff (1967): Soil toxomony, U.S. Department of Agriculture, Washington DC.

The Software Toolworks, Inc. (1991-1994):World Atlas ver.4 [CD-ROM]

Traore H., et, al (1978). Plan minéral de la République du Mali. Direct. Nat. min., geol., Bamako, BRGM, 631p.

Tropical soils, 3rd edition Mouton,

Vinchon C. et, al (1986) : Caractérisation lithostructurale de deux ensembles successifs dans les séries birrimiennes de lq boutonniére de Kédougou (Mali-Sénégal) et du Niandan (Guinée) ; implications gitologiques. CIFEG, publication occasionnelle, n 10, pp. 113-121

Zang, W. and Fyfe, W.(1993) : A Three-Stage Genetic Model for the Igarapé Behia Lateritic Gold Deposit, Carajàs, Brazil. Eco. Geo., vol88, num7, p1768

Zeegers H.and Leduc C.(1991): Geochemical exploration fro gold in temerate, arid and tropical rain forest terrains. In Gold metallogeny and exploration. Foster R.P. (Glasgow: Blackie,1991), 309-35.

Zelssink, H. E, (1969) : The Mineralogy and Geochemistry of a Nickeliferous Laterite Profile (Greenvale, Queensland, Australia) : Mineralium Deposita, v. 4, p. 132-152.

Appendice

Apc.1 Résultat d'observation microscopique en lames minces

Apc.1 Résultat d'observation microscopique en lames minces (1/2)

	Sample number	Rock name	Quartz	Alkali feldspar	Plagioclase	Biotite	Muscovite	Hornblende	Augite	Hypersthene	Olivine	Apatite	Zircon	Spinel	Opaque minerals	Epidote	Actinolite	Tremolite	Garnet	Sphene	Tourmaline	Chlorite	Sericite	Smectite	Calcite
1	AH-1	sandy biotite hornfels	++	+	+	++							(+)		+										(+)
2	AH-2	conglomerate hornfels	+++	++	+	++									(+)										(+)
3	AH-4-2	conglomerate hornfels	++	++	+	++							(+)		(+)							+			
4	BR-2	meta-granite	+	++	++								(+)			+						+		+	
5	KN-2-3	biotite granite	+	++	+	+						(+)			(+)										
6	KN-2-4	dolerite	(+)	(+)	+++	(+)			+	+					+									(+)	
7	KR-1	quartz vein, with tourmaline	++												(+)						+++				
8	MAB-50	hornblende biotite granodiorite	+	+	+++	++	(+)	+				(+)	(+)		+			+					+		
9	MAF-170	meta sandstone	+++										(+)			++		+				+	+		+
10	MAG-940-3	meta sandstone	+++				+	+				(+)			+		+					(+)			+
11	MB-150-3	tourmaline schist	+++				+								(+)						+		++		
12	MB-150-4	tourmaline hornfels	++												+						+++				
13	MB-50-2	hornblende biotite granite	++	++	+	++	(+)	+				(+)	(+)									+	+		
14	MC-100-2	hornblende biotite granite	++	++	++	+	(+)	+				(+)	(+)									+			
15	MC-315	biotite granodiorite	++	+	+++	++	(+)	+				(+)	(+)									+			
16	MC-400-3	meta quartzite	+++												+										
17	MD-130	tourmaline schist	++												+						+++				
18	MF-275-2	mica schist	++				++																++		+
19	MM-125	meta sediment & quartz vein	++				+							+	+						+++				
20	MO-400-2	hornblende biotite granodiorite	++	+	++	++	(+)	+				(+)	(+)		+								++		
21	MS-70	dolerite	+	+	+++	+			+++			(+)			+								+		
22	MU-350	biotite granite porphyry	++		+++	++	++	++				(+)											+	+		+
23	MU-975	conglomerate biotite hornfels	+++		+	++							(+)		(+)										
24	Nag-1	actinolite bearing meta-sandstone	++		+												++		+	(+)		(+)			
25	Nag-3	silicified quartz dacite	+++		+	(+)	+								+										
26	Nag-5	sandy biotite hornfels	++	++	++	++						(+)			(+)										
27	R-707	silicified quartz dacite, quartz vein	+++		+		+								+										
28	RAQ-683750	two mica granite	++	++	++	+	+					(+)	(+)									(+)			

+++ : abundant (>30%)
++ : common (10-30%)
+ : little (1-10%)
(+) : rare (<1%)

Apc.1 Résultat d'observation microscopique en lames minces (2/2)

	Sample number	Rock name	Quartz	Alkali feldspar	Plagioclase	Biotite	Muscovite	Hornblende	Augite	Hypersthene	Olivine	Apatite	Zircon	Spinel	Opaque minerals	Epidote	Actinolite	Tremolite	Garnet	Sphene	Tourmaline	Chlorite	Sericite	Smectite	Calcite
29	RAR-699980	mica schist	++		++	+++	++					(+)	(+)									+			
30	RAW-676100	dolerite			+++				+++		(+)				+									+	
31	RAW-680150	dolerite			+++	(+)			+++						+									+	
32	RAX-679550	two-mica granite	+++	+	++	+	+					(+)	(+)									+	(+)		
33	RAX-707800	dolerite	(+)	(+)	+++	+			++	+					+							+		+	
34	RAZ-691700	garnet-actinolite schist	++		+												++		+	+					
35	RBE-697870	granite porphyry	++	+	+++	++		++				(+)	(+)		+	(+)									
36	RBF-692650- 3	sandy garnet-mica hornfels	++				++						(+)			++			+	(+)			+		
37	RBF-698100	dolerite	(+)	(+)	+++	+		+	++	++					+							(+)		+	
38	RBK-696700	altered dolerite	(+)	(+)	+++	(+)		+	++	+		(+)	(+)		+							+	+	+	
39	RBL-697500	biotite hornfels	++			++							(+)		+						(+)				
40	RCP-618100	sandy biotite hornfels	+++		++	++							(+)									+			
41	RCS-617250	biotite granite	++	++	+	++	+						(+)		(+)								(+)	(+)	
42	RCS-617250	sandy biotite hornfels	+++		++	++																+			
43	RMR-22010	tourmaline bearing quartz vein rock	++	+			++					+									++				

+++ : abundant (>30%)
++ : common (10-30%)
+ : little (1-10%)
(+) : rare (<1%)

(1) AH-1
Sandy biotite hornfels
Original rock is poory sorted alkose sandstone. Grains are composed of quartz and feldspars up to several mm. Secondary minerals in the groudmass comprise biotite ,small amounts of calcite and opaque minerals.

(2) AH-2
Conglomerate hornfels
Original rock is poorly sorted breccia. Breccias comprise quartz, feldspars and altered (silicified) volcanics. Aggregates of biotite and smectite are also observed in and around these grains.

(3) AH-4-2
Conglomerate hornfels
Original rock is poorly sorted breccia, comprising quartz, feldspars (volcanic origin) and mudstone. Fine grains of biotite and small amount of chlorite are observed in and around the matrix.

(4) BR-2
Meta-granite
Coarse grained altered granite. Mafic minerals are totally altered to biotite, epidote and clay minerals. Epidote is fine grained with up to 0.5 mm.

(5) KN-2-3
Biotite granite
Coarse grained equigranular biotite granite. Feldspars which exhibit weak zoning are weakly altered, with fine grains of secondary minerals. Quartz exhibits wavy extinction. In and around the grains of biotite, opaque minerals are observed.

(6) KN-2-4
Dolerite
This rock is composed of coarse grains of hypersthene (up to several mm), plagioclase and augite. Hypersthene and plagioclase are euhedral or subhedral, and augite is anhedral on the other hand. Hypersthene grains are suffered some alteration, with small amount of clay minerals. Some amounts of alteration minerals (smectite) and opaque minerals are recognized in the interstices of phenocrysts.

(7) KR-1
Quartz vein, with tourmaline
Fine grains of tourmaline accompanying small amounts of opaque minerals up to 1mm in diameter are arranged in strong orientation. With distinct boundary, coarse grains of tourmaline are hosted by very coarse quartz grain.

(8) MAB-50
Hornblende Biotite Granite
Coarse (2-4mm) grain tabular plagioclase is surrounded by finer quartz. Plagioclase has zoning with some amount of altered minerals. Quartz shows weak wavy extinction. Colored minerals are biotite and hornblende. Accessory minerals are zircon and apatite. The dark inclusion bearing needle-shape tremolite and quartz (several mm).

(9) MAF-170
Meta Sandstone
Poorly sorted, poorly rounded quartz is cemented by epidote and fine grain calcite. Quartz grain originated from coarse grain equigranular granitic rocks. There are tremolite, muscovite and zircon as accessory minerals.

(10) MAG-940-3
Meta Sandstone
Poorly sorted, poorly rounded quartz, which diameter ranged from 1mm to micron-scale, is dominant member. The very fine quartz grains are gathered with muscovite. This aggregate cements crastic grain. Radial needle-like actinolite is seen. Quartz grain originated from grainitic rocks.

(11) MB-150-3
Tourmaline Schist
Euhedral tourmaline with 0.5-3mm length are scattered and among them fine grain quartz cement. Finer muscovite cement the quartz grains. Muscovite sometimes makes aggregates.

(12) MB-150-4
Tourmaline hornfels
There are tabular grains of tourmaline with 50um diameter and 1mm length, and with no orientation of crystal. Among the tourmaline there are quartz and other minerals, which are not obscure under the microscope. Quartz aggregate is seen in some places.

(13) MB-50-2
Hornblende Biotite Granite
Coarse (2-4mm) grain tabular plagioclase and K-feldspar are surrounded by finer quartz. Plagioclase has zoning with some amount of altered minerals. Quartz shows weakly wavy extinction. Colored minerals are biotite and hornblende. Hornblende usually makes aggregates together with biotite.

(14) MC-100-2
Hornblende Biotite Granite
Coarse (2-4mm) grain tabular plagioclase is surrounded by finer (-1mm) quartz and plagioclase. Plagioclase has zoning with some amount of altered minerals. Quartz shows weak wavy extinction. Colored minerals are biotite and hornblende. Hornblende makes aggregates together with biotite. The mafic inclusion bearing smaller plagioclase with higher mode of colored minerals.

(15) MC-315
Biotite Granodiorite
Coarse (2-4mm) grain tabular plagioclase and K-feldspar are surrounded by finer quartz, plagioclase and K-feldspar. Plagioclase has zoning with some amount of altered minerals. Quartz shows weakly wavy extinction. Colored minerals are biotite and green hornblende. Small amount of apatite is seen as inclusions in quartz.

(16) MC-400-3
Meta Quartzite
Almost all volume is consists of quartz which shows strongly wavy extinction. In some places, quartz partly having subgrain is seen. The grain boundary becomes complicated. A very small quantity of opaque mineral concentrates.

(17) MD-130
Tourmaline schist
Tabular tourmaline makes foliation. And parallel to this foliation the layer concentrated in fine quartz or tourmaline. This layer is not so continuous. Tourmaline has many inclusions. There are some opaque minerals in the grain boundary between quartzes.

(18) MF-275-2
Mica schist
Fine grain quartz and mica are dominant minerals. Quartz and mica make foliation by their ratio. Some detrial quartz grain is seen. Some place is partly replaced by calcite.

(19) MM-125
Meta sandstone & Quartz vein
Poorly sorted quartz sandstone with metamorphic fine grain tabular tourmaline. The quartz grain shows strongly wavy extinction. The small amount of muscovite and spinel are seen. Quartz vein is consists of course grain quartz and tourmaline. The tourmalines at the grain boundary of quartz are coarser grain than in host rock, and have tabular shape.

(20) MO-400-2
Hornblende Biotite Granodiorite
Coarse (2-4mm) grain tabular plagioclase and orthoclase are euhedral surrounded by quartz. These feldspar have zoning with some amount of altered minerals (muscovite). The zoning of these minerals is weak. Quartz shows weakly wavy extinction. Accessory minerals are zircon and apatite.

(21) MS-70
Augite dolerite
Aphyric dolerite. The groundmass consists of semi-euhedral plagioclase and augite with several 100 micro m. No significant flow texture is observed. Interstitial spaces are filled with biotite, which are partly replaced with chlorite.

(22) MU-350
Biotite granite porphyry

Phenocryst minerals are mainly plagioclase with about 1mm length. Groundmass consists with quartz, plagioclase, and biotite less than 0.1mm in diameter. Some biotite make clot ca. 1mm. Dark colored enclaves consist with fine-grained biotite and plagioclase. Plagioclases are partly replaced with sericite and other secondary minerals. Groundmass has small amount of calcite. Biotites are partly replaced with chlorite.

(23) MU-975
Conglomerate biotite hornfels

Poorly sorted fine-grained breccia. Clasts mainly consist with silicified volcanic rocks and pelitic rocks. Matrix consists with poorly sorted fragments of quartz and plagioclase. Fine-grained secondary biotite and calcite occur in matrix part.

(24) Nag-1
Actinolite bearing meta-sandstone

Original rock is supposed to be poorly sorted sandstone, comprising quartz, K-feldspar and actinolite exhibiting fibrous texture with minor amount of epidote. These minerals are cemented by fine grains of silica minerals due to silicification. Secondary minerals are recognized in the grains of K-feldspar.

(25) Nag-3
Silicified quartz dacite

Strongly silicified dacite. Only the phenocrysts of quartz and feldspars are preserved due to silicification. Inside and around the crystals of feldspars, secondary minerals are observed. Coarse grains of opaque minerals are scattered.

(26) Nag-5
Sandy biotite hornfels

Original rock is poorly sorted sandstone. Grains are composed of quartz, feldspars, mudstone, opaque mineral and minor amount of zircon. Alteration minerals are mainly biotite, with minor amount of secondary mineral in the feldspars.

(27) R-707
Silicified quartz dacite, quartz vein

Intensely silicified dacite contacts distinctly with quartz vein. Only the phenocrysts of quartz and feldspars are remained due to strong silicification. Garnet and some silica minerals are observed. Quartz vein is composed of coarse grains of quartz and minor amount of opaque mineral.

(28) RAQ-683,750
Two-mica granite

Coarse grained granite bearing both biotite and muscovite. Plagioclase crystals show weak compositional zoning. Mica and quartz crystal sometimes exhibit wavy extinction. Small amount of zircon and apatite are bearing.

(29) RAR-669,980
Mica schist

Tabular biotite show strongly preferred orientation. Interstitial parts are filling with fine-grained quartz and plagioclase. Biotite and quartz exhibit weak wavy extinction. Lens- shaped spots with coarse quartz, biotite, and muscovite are observed.

(30) RAW-676,100
Dolerite

Fine-grained aphyric dolerite consists with semi - euhedral plagioclase and augite. Small amount of (less than 1 volume %) olivine pseudomorphs replaced with smectite are bearing. Weakly alteration are observed along thin smectite vein.

(31) RAW-680,150
Dolerite

Fine-grained aphyric dolerite consists with semi-euhedral plagioclase and augite. The length of tabular plagioclase are about 400 micrometer and they are slightly larger than sample RAW 676,100. No olivine is bearing. Very small amounts of biotite fill interstitial space. Small amounts of secondary minerals are observed in plagioclase.

(32) RAX-679,550
Two-mica granite

Coarse grained equigranular granite with biotite and muscovite. Plagioclase exhibits weak compositional zoning. Muscovites mainly occur inside plagioclase crystals. Quartz and biotite exhibit wavy extinction. Biotites are partly replaced with chlorite and core parts of plagioclase bearing very fine-grained secondary minerals.

(33) RAX-707,800
Dolerite

Coarse grained dolerite consists with hypersthene, plagioclase, and augite. Hypersthene crystals are larger than plagioclase and augite crystals. Plagioclase shows compositional zoning. Interstitial spaces between these minerals are filled with myrmekite. Hypersthene crystals are partly replaced along cracks. Some augites are partly replaced with very fine grained secondary minerals.

(34) RAZ-691,700
Garnet-actinolite schist

Poorly sorted alkose sandstone with low grade metamorphism. Radial clots of actinolite with 1mm length are developed. Small amount of metacryst garnets occur.

(35) RBE-697,870
Granite porphyry

Phenocrysts are plagioclase with 0.5-5mm length, biotite and hornblende with 0.5mm. Phenocrysts plagioclases exhibit remarkable normal zoning. Biotite and hornblende sometimes consists clots with several mm in diameter. Groundmass consists quartz, alkali feldspar, plagioclase, biotite, and hornblende. Small amounts of zircon and apatite are bearing. Plagioclase crystals are partly replaced with fine grained secondary minerals (epidote and fine-grained clay minerals).

(36) RBF-692,650-3
Sandy garnet-mica hornfels

Original rocks are poorly sorted, coarse grained sandstone. Primary minerals expect quartz are replaced with metamorphic minerals, which are epidote with 0.1mm length, garnet with 0.2-0.4mm, and fine grained muscovite. Small amount of sphene are bearing.

(37) RBF-698,100
Dolerite

Coarse grained dolerite with hypersthene, plagioclase, augite, and hornblende. Hypersthene and plagioclase show euhedral shapes. Plagioclases exhibit remarkable compositional zoning. Interstitial spaces between these minerals are filling with myrmekite. Hypersthene crystals are partly replaced along cracks. Some augites and plagioclases are partly replaced with very fine grained secondary minerals.

(38) RBK-696,700
Altered dolerite

This sample is similar to RBF 698,100, but more coarse grained ($1 \sim 2$ mm) . Coarse grained dolerite with euhedral shaped hypersthene, plagioclase, augite, and hornblende. Plagioclases exhibit remarkable compositional zoning. Interstitial spaces between these minerals are filling with biotite and myrmekite. Hypersthene crystals are partly replaced along cracks. Some augites and plagioclases are partly replaced with very fine-grained secondary minerals. Very fine-grained secondary minerals occur in pyroxenes and plagioclase. Marginal parts of biotite and hornblende crystals are replaced with chlorite, some of them show hexagonal euhedral crystals.

(39) RBL-697,500
Biotite hornfels

This sample consists of preferred orientated biotite and quartz grains with several 10 micrometers. Biotite and quartz exhibit remarkable wavy extinction. Very small amounts of tourmaline are bearing. A quartz vein across this sample.

(40) RCP-618,100
Sandy biotite hornfels

Poorly sorted alkose sandstone with weak alteration. Constituents except for quartz and K-feldspar (up to several mm) are replaced by altered minerals. Altered minerals are composed of aggregates of biotite and chlorite. Small amounts of zircon are also observed.

(41) RCS-617,250-1
Sandy biotite hornfels
Pooly sorted alkose sandstone with weak alteration. Grains are composed of quartz and small amounts of K-feldspar (up to several mm), with small amounts of altered minerals comprising biotite and clay minerals (smectite).

(42) RCP-617,250
Altered quartz dacite
Strongly altered dacite. Only the vestiges of phenocrysts of quartz and feldspars are remained due to strong alteration. Aggregates of biotite are in the voids, and scattered grains of that are in the groundmass. Secondary minerals (muscovite?) are in the feldspars.

(43) RMR-22,010
Tourmaline bearing quartz vein rock
There observed two parts, tourmaline part and quartz part. Strong orientation of tourmaline grains, cemented by muscovite, quartz and opaque minerals is recognized in the tourmaline part. Muscovite grains (up to several mm) are observed in the interstices of coarse grains of quartz.

Sample No.: MF-275-2
Rock name: mica schist
Location: Secteur B, Kekoro
ms:Muscovite, qz:Quartz

Open nichols

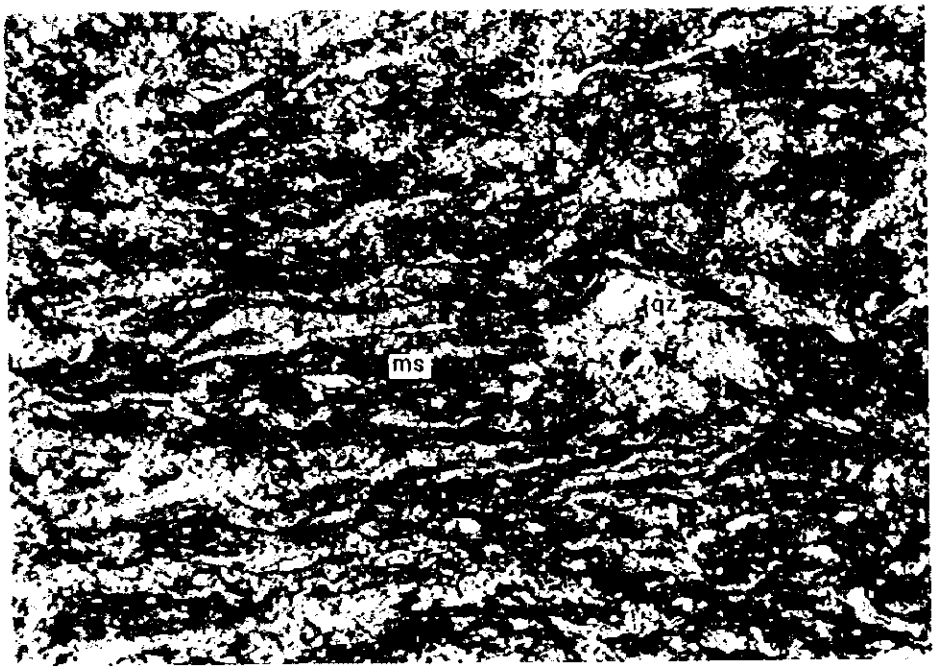

Cross nichols

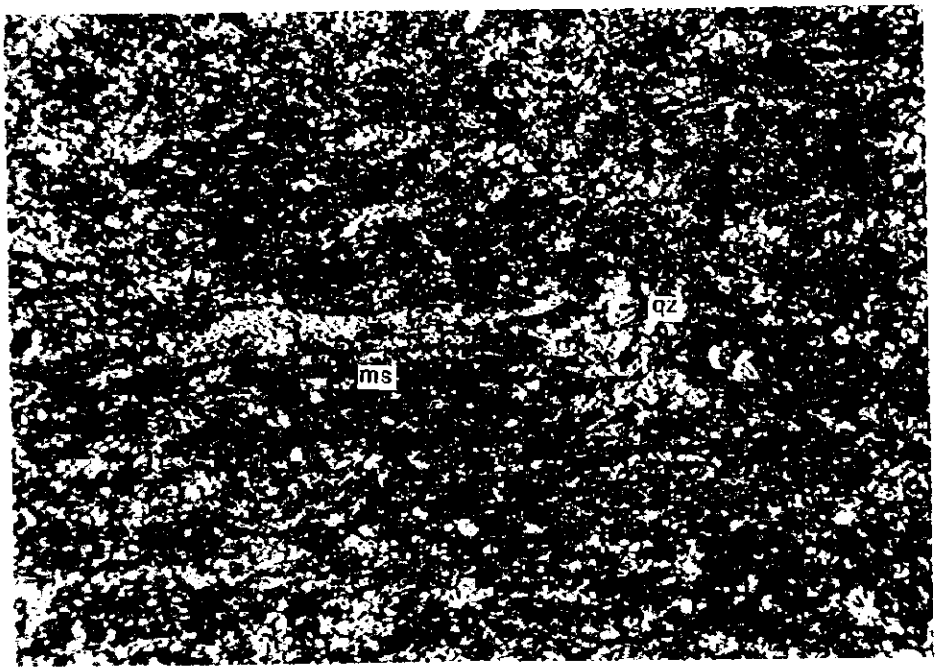

1mm

Sample No.: RAR-699980
Rock name: mica schist
Location: Baoule-Banifing
qz:Quartz, ms:Muscovite, bi:Biotite, chl:Chlorite

Open nichols

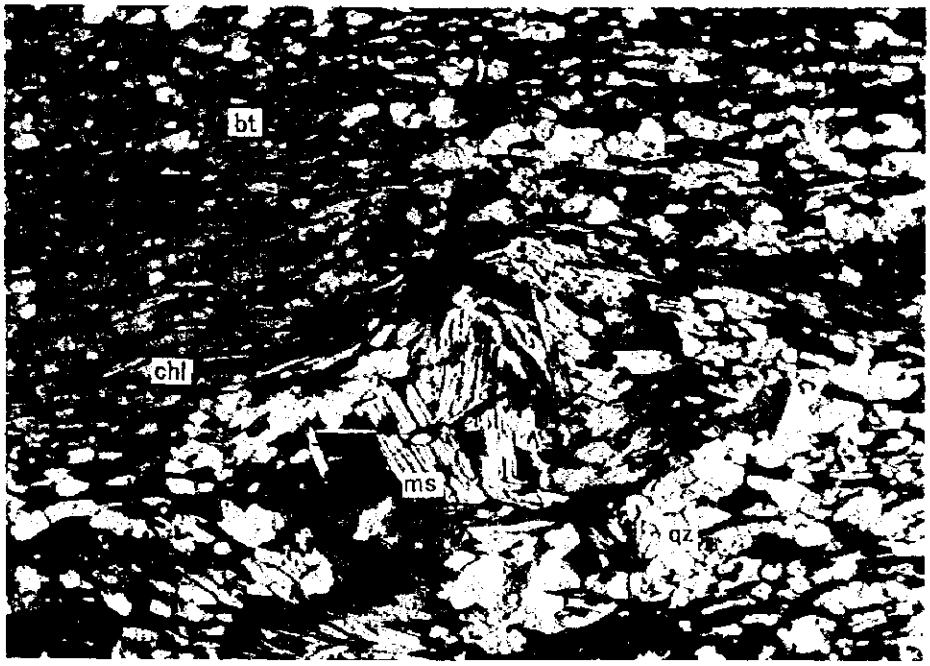

Cross nichols

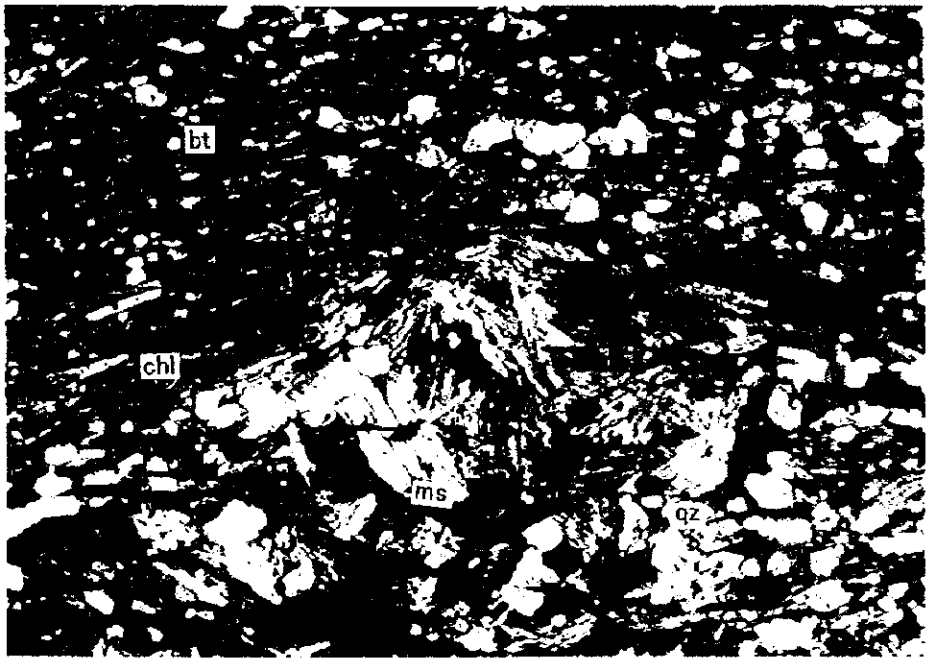

1mm

Sample No.: RBL-697500
Rock name: biotite hornfels
Location: Baoule-Banifing
qz:Quartz, bt:Biotite, zr:Zircon

Open nichols

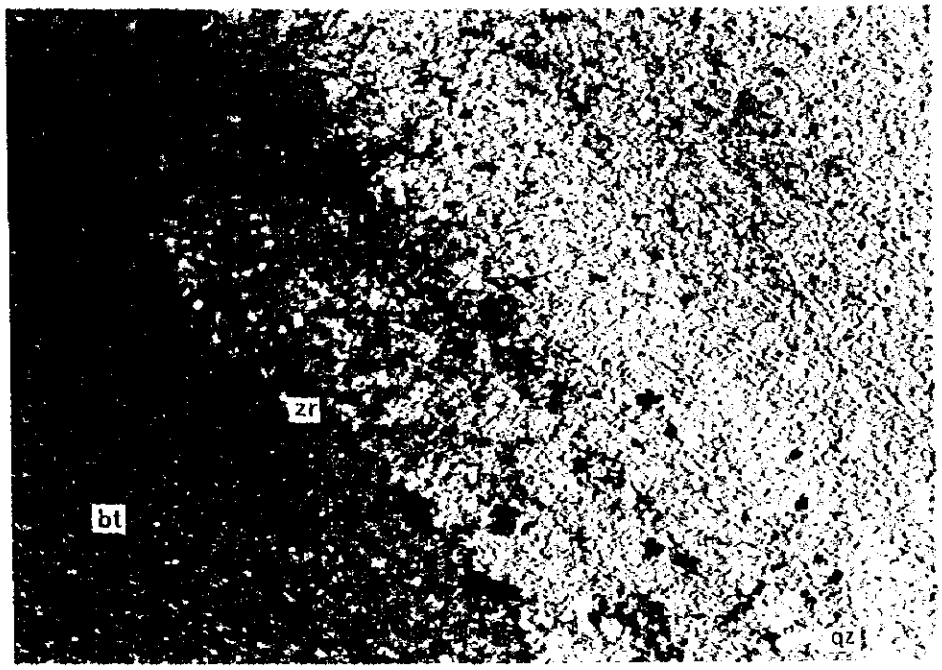

Cross nichols

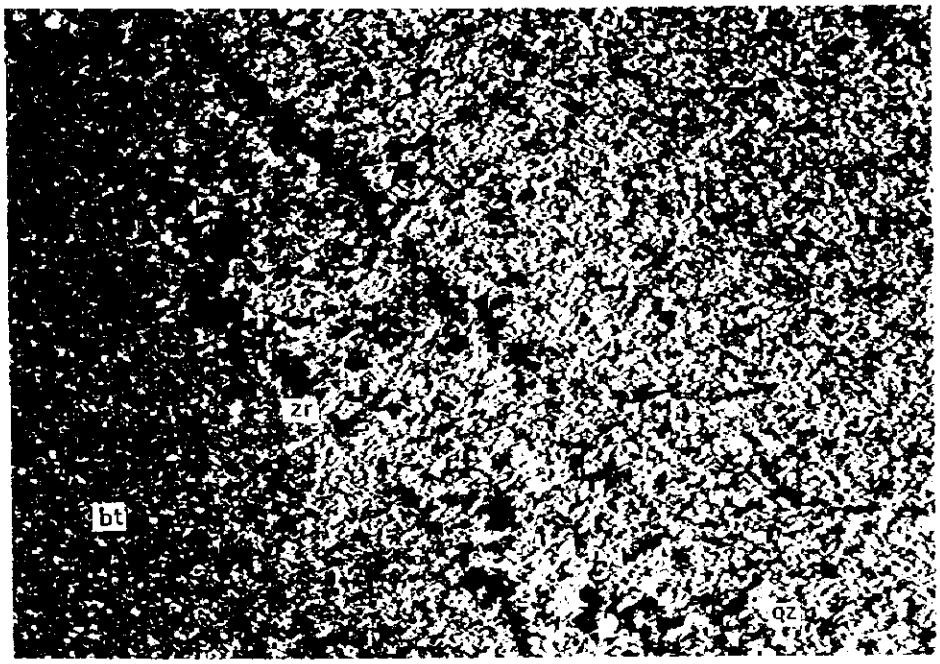

1cm

Sample No.: Nag-5
Rock name: biotite hornfels, sandy
Location: Secteur E, Kekoro
pl:Plagioclase, or:Orthoclase, qz:Quartz

Open nichols

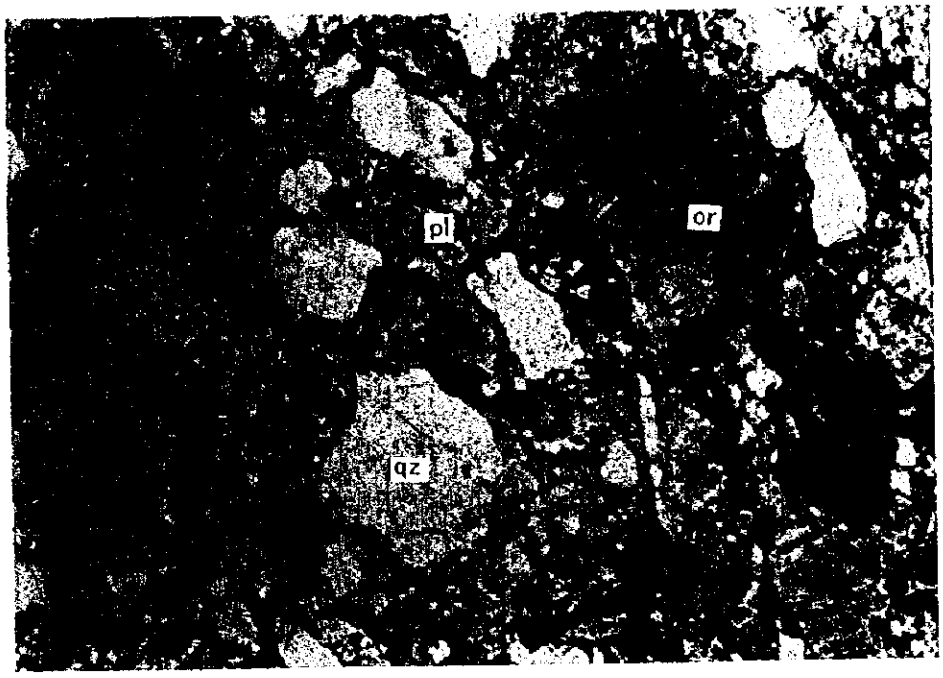

Cross nichols

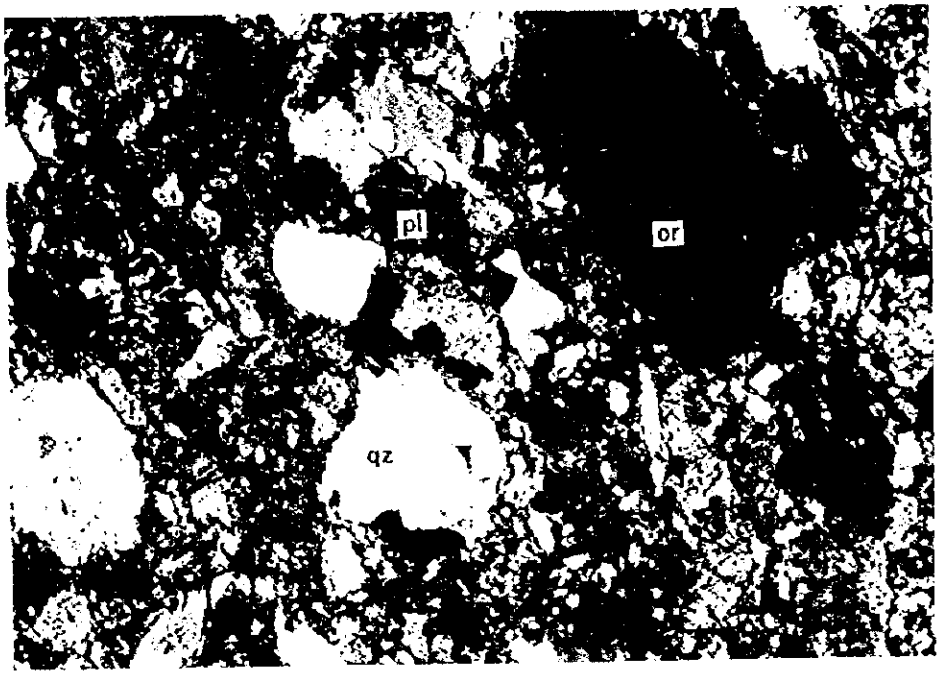

Sample No.: RCP-618100
Rock name: biotite hornfels, sandy
Location: Baoule-Banifing
qz:Quartz, or:Orthoclase, chl:Chlorite

Open nichols

Cross nichols

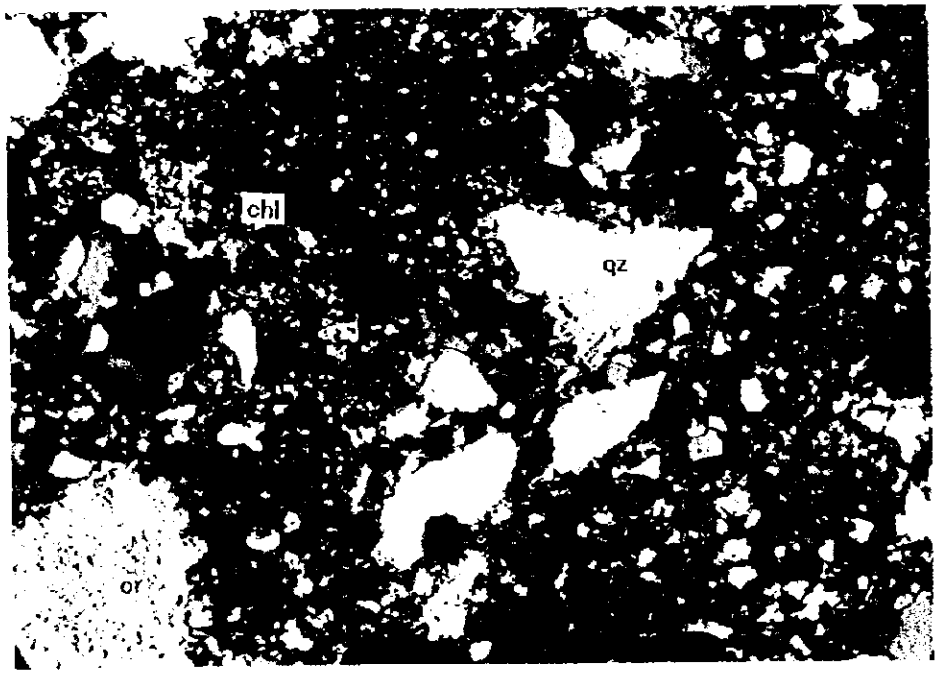

1mm

Sample No.: MD-130
Rock name: tourmaline schist
Location: Secteur B, Kekoro
tm:Tourmaline, qz:Quartz

Open nichols

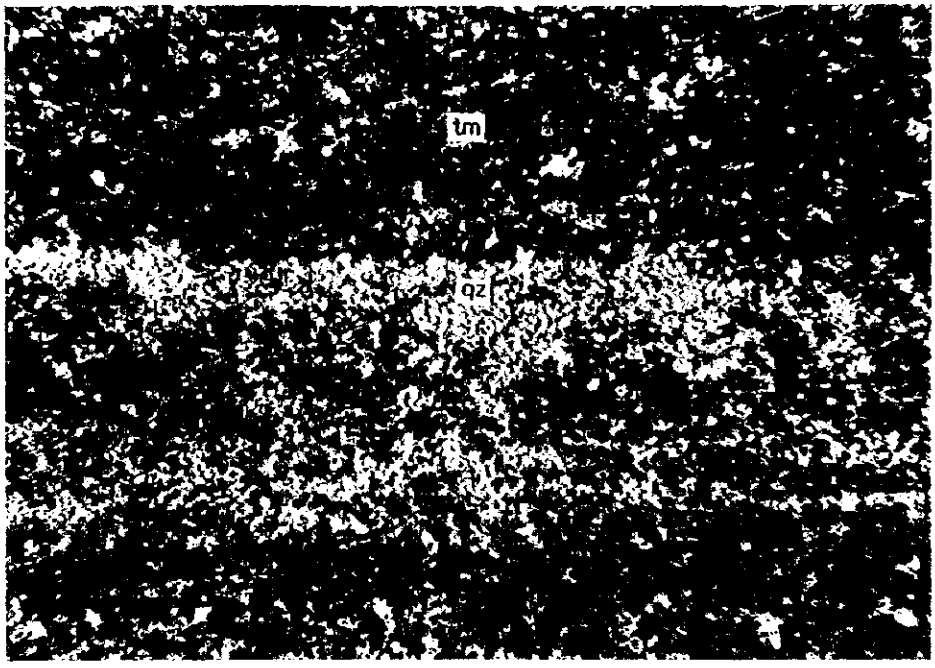

Cross nichols

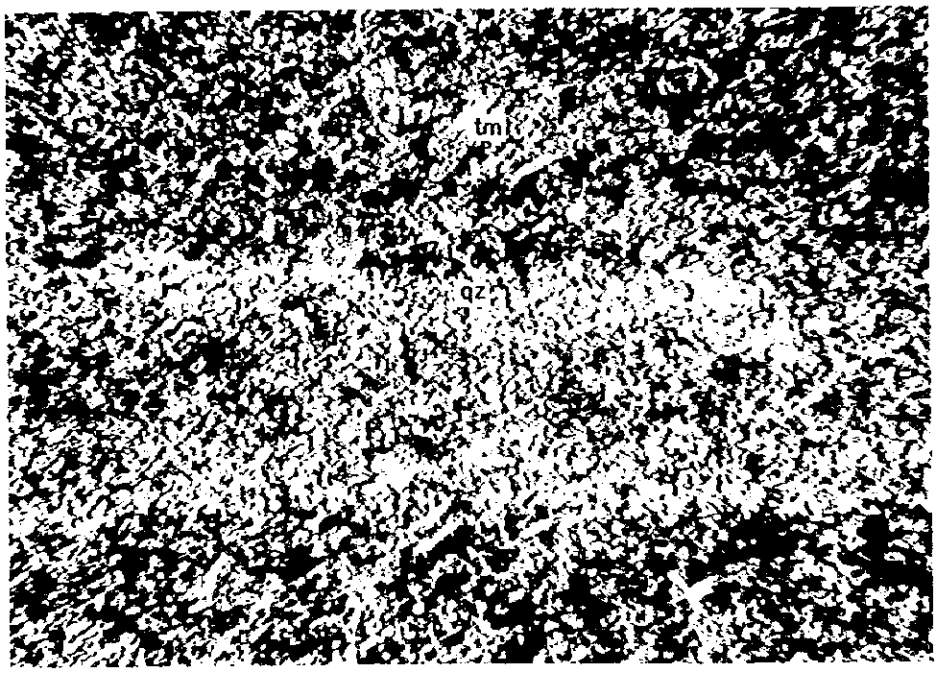

Sample No.: MB-150-4
Rock name: tourmaline hornfels
Location: Secteur A, Kekoro
tm:Tourmaline

Open nichols

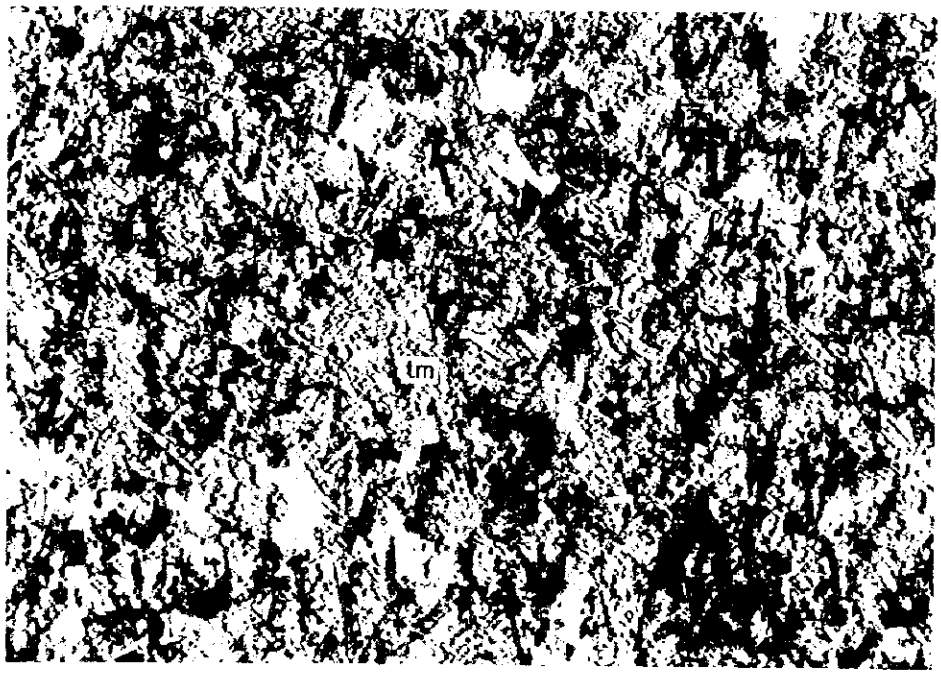

Cross nichols

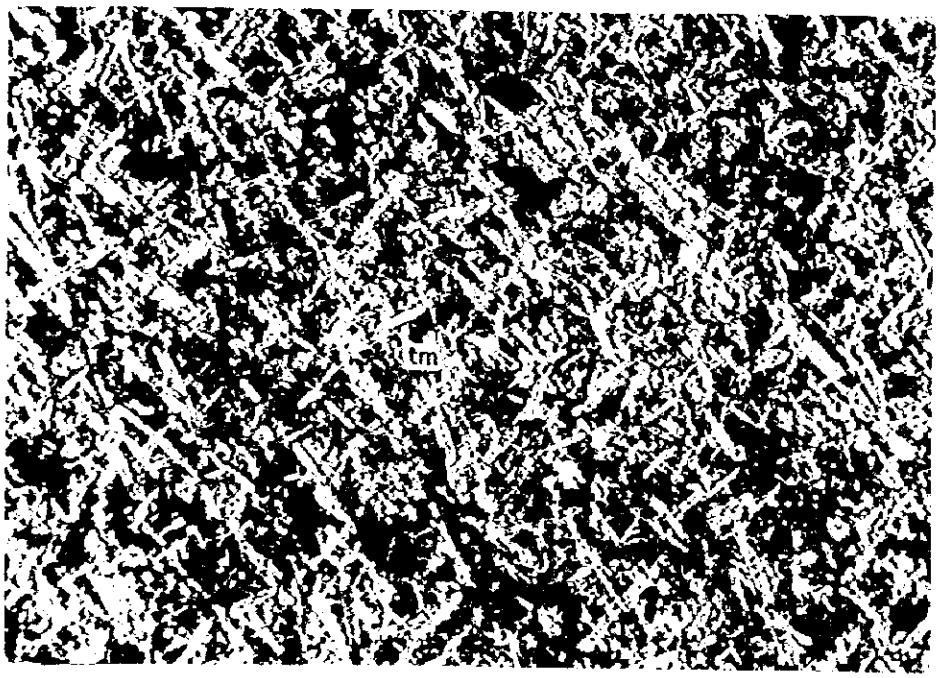

1mm

Sample No.: Nag-3
Rock name: silicified dacite
Location: Secteur E, Kekoro
pl:Plagioclase, qz:Quartz

Open nichols

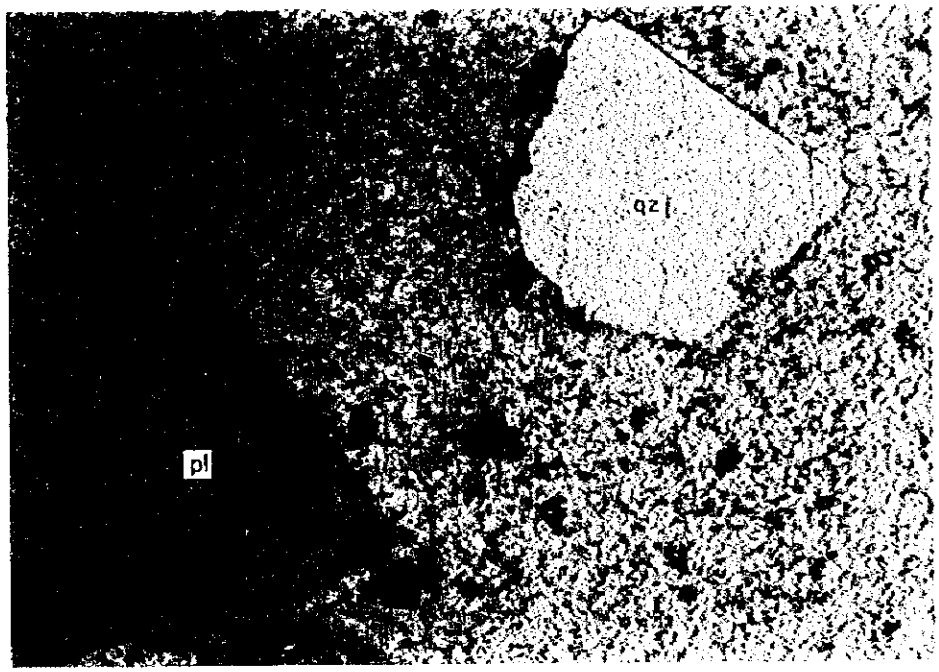

Cross nichols

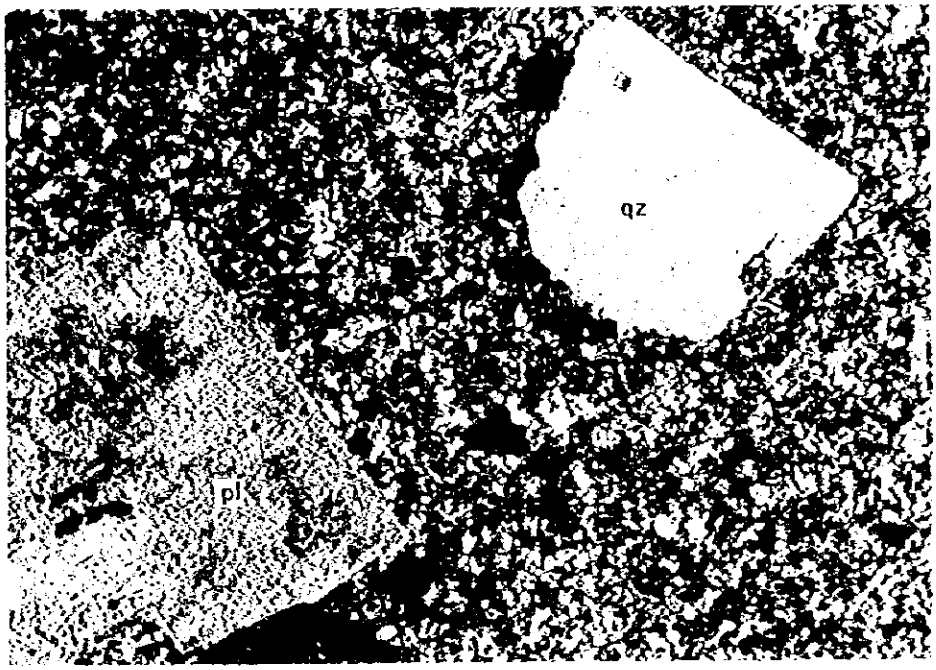

Sample No.: RBE-697870

Rock name: granite porphyry

Location: Baoule-Banifing

pl:Plagioclase, or:Orthoclase, qz:Quartz, hb:Hornblende, bi:Biotite

Open nichols

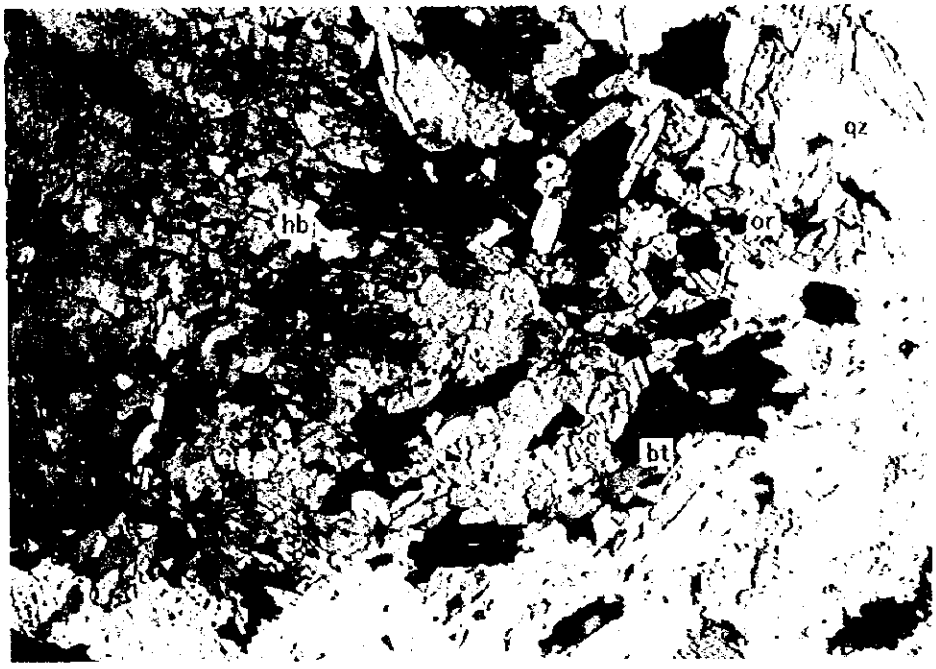

Cross nichols

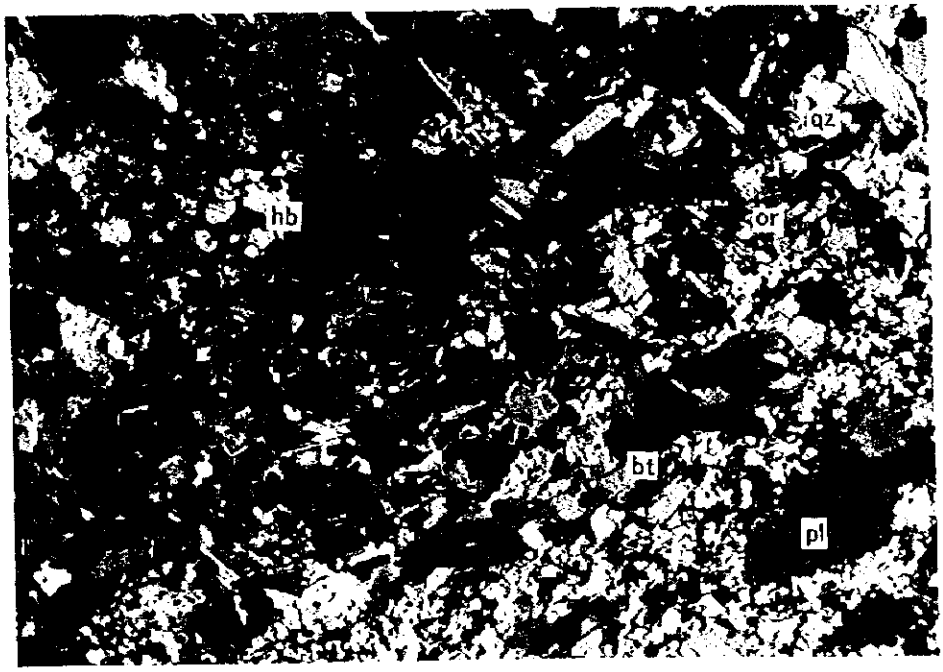

1mm

Sample No.: RAX-679550

Rock name: two-mica granite

Location: Baoule-Banifing

pl:Plagioclase, or:Orthoclase, qz:Quartz, ms:Muscovite, bi:Biotite

Open nichols

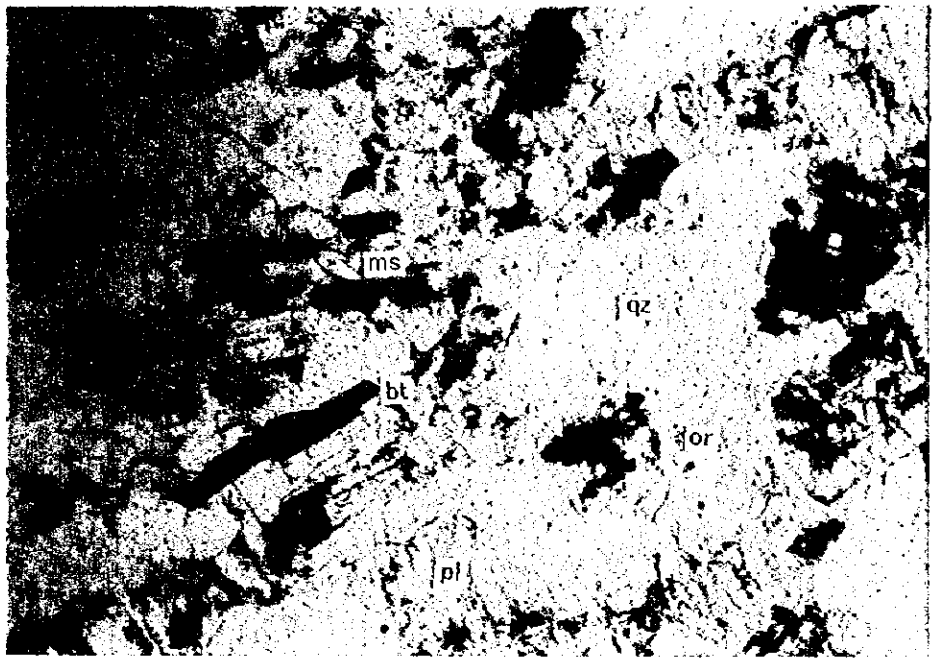

Cross nichols

1mm

Sample No.: RAX-707800
Rock name: dolerite
Location: Baoule-Banifing
hyp:Hypersthene, au:Augite, pl:Plagioclase

Open nichols

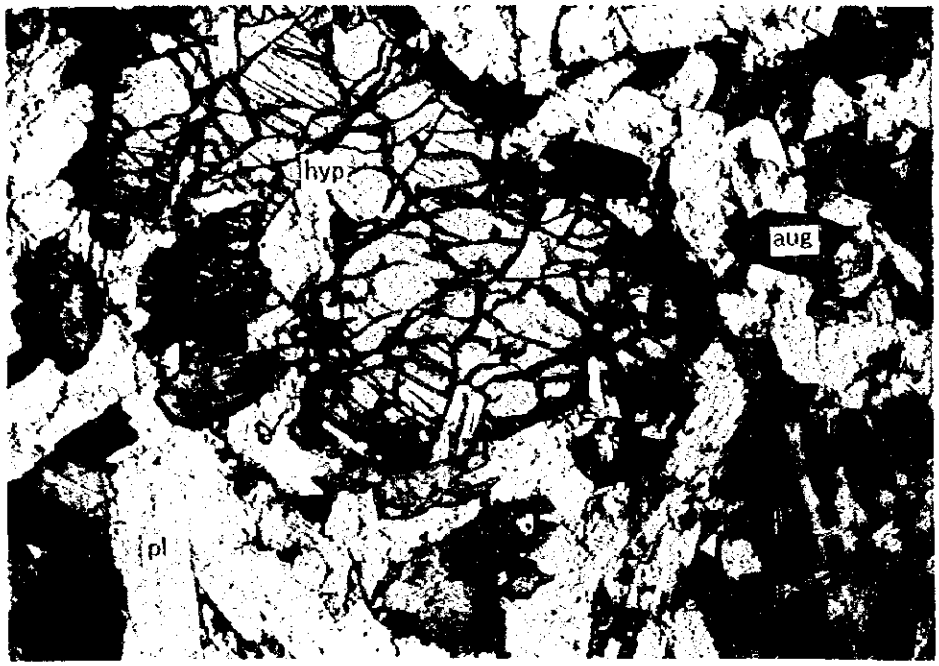

Cross nichols

1mm

Sample No.: KR-1
Rock name: quartz vein with tourmaline
Location: Kouloukoro
tm:Tourmaline, qz:Quartz

Open nichols

Cross nichols

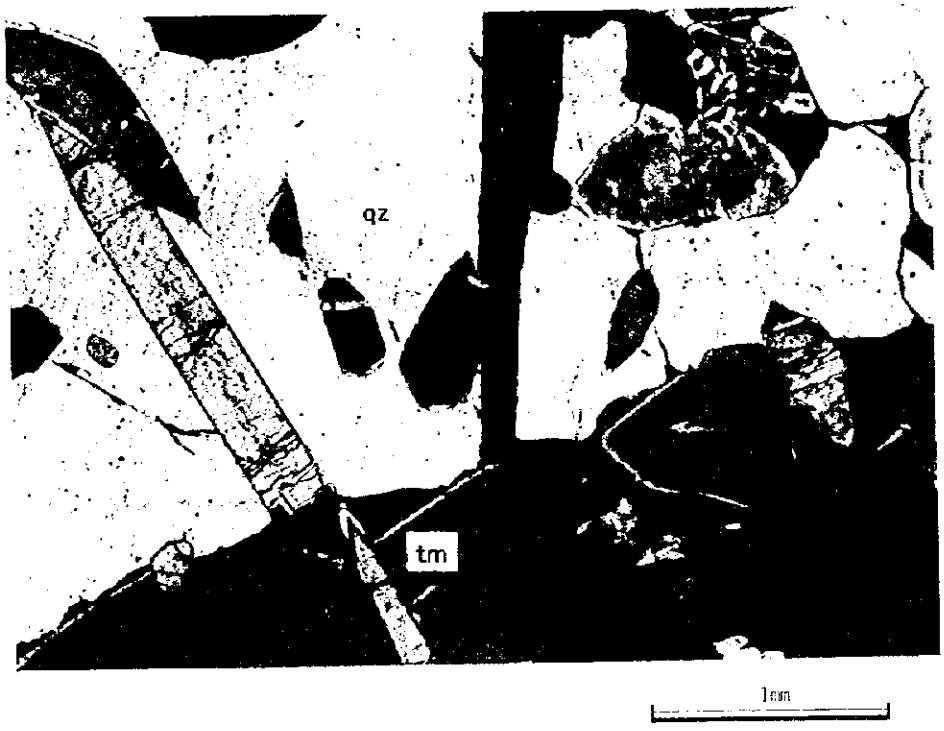

Apc.2 Résultat d'observation microscopique en lames polies

Apc.2 Résultat d'observation microscopique en lames polies (1/4)

1	MAG-940-3 meta-sandstone Area: Kékoro	This polished section is composed of pyrrhotite (50 %), pyrite (30 %), chalcopyrite (10 %), ilmenite (5 %), goethite (5 %) and gangue minerals. Pyrrhotite occurs as aggregates of anhedral grains up to 0.7 mm in size, and some grains of it changed into pyrite, especially in the marginal parts and along the cracks. Pyrite occurs as euhedral to subhedral grains in the marginal parts of the pyrrhotite aggregates and as anhedral grains that possibly replaced pyrrhotite under higher sulfur fugacity in the later stage. Chalcopyrite shows veinlets of 20 to 30 μm in width in pyrrhotite. Ilmenite may be one of the primary constituent minerals of fine-grained dolerite. Goethite is a secondary product of alteration possibly after pyrite, based on its shape.
2	MB-125 quartz float Area: Kékoro A	The opaque minerals are rare in this polished section. It consists of carbonaceous matters (90 %), pyrite (10 %) and gangue minerals. The carbonaceous matters occur as irregular-shaped (amoeboid) aggregates up to 40 μm in size. Pyrite occurs as subhedral to anhedral grains up to 10 to 20 μm in size.
3	MB-150-2 quartz float Area: Kékoro A	This polished section is composed of carbonaceous matters (50 %), goethite (25 %), pyrite (20 %), hematite (5 %) and gangue minerals. The carbonaceous matters occur as irregular-shaped, amoeboid aggregates like No. 2 sample (MB 125). Goethite occurs as cube-shaped aggregates of very fine grains that probably shows psuedomorph after pyrite, and includes anhedral grains of hematite. Pyrite occurs as descrete, subhedral grains of 40 μm in size.
4	MC-200-2 dolerite dissseminated by pyrite Area: Kékoro	This consists of goethite (50 %), ilmenite (30 %), hematite (15 %), pyrite (5 %) and gangue minerals. Goethite occurs as massive, irregular-shaped aggregates up to 0.2 mm in size and as cube-shaped aggregates of very fine grains that probably shows psuedomorph after pyrite. Ilmenite may be one of the primary constituent minerals of dolerite. Hematite occurs as needle-shaped crystals of approximate 50 μm in length. Ilmenite and hematite are frequently rimmed by goethite. Also in the central parts of the goethite aggregates, anhedral to subhedral, rounded grains of pyrite up to 30 μm in size are sometimes observed.
5	MC-290 quartz float Area: Kékoro	This polished section is composed of pyrite (97 %) and a lesser amount of "electrum" (3 %) with a lot of gangue minerals. Pyrite occurs as rounded grains up to 20 μm in size. "Electrum" rarely occurs as iregular-shaped grains up to 20 μm in size. Because the color of the "electrum" is bright creamy white, it should contain some contents of silver.
6	MC-320 quartz float Area: Kékoro A	It is composed of goethite (50 %), carbonaceous matters (30 %), pyrite (20 %) and gangue minerals. Goethite occurs as aggregates of fine grains, and includes rounded pyrite grains of approximate 10 μm in size.
7	MC-400-3 quartz float quartzite ?? Area: Kékoro B	This is also composed of large amounts of gangue minerals, and the opaque minerals are rare. The opaque minerals are carbonaceous matters (97 %) and "electrum" (3 %). The carbonaceous matters occur as aggregates of tiny grains up to several μm in size, each of them showing very soft hardness and strong anisotropism. "Electrum" occurs iregular-shaped grains up to 10 μm in size, and maybe Au-rich on the basis of its reflectant color.
8	MC-625-2 smoky quartz float Area: Kékoro B	This polished section consists of pyrite (70 %), carbonaceous matters (27 %), "electrum" (3 %) and gangue minerals. Pyrite is descrete, euhedral to subhedral, and the carbonaceous matters is descrete, anhedral. "Electrum" occurs as anhedral grains up to 10 μm in size.

Apc.2 Résultat d'observation microscopique on lames polies (2/4)

9 MC-650-2 smoky quartz float Area: Kékoro B	It is composed of carbonaceous matters (80 %), pyrite (10 %), goethite (10 %) and gangue minerals. The carbonaceous matters occurs as discontinuous veinlets up to 0.2 mm in width. Pyrite occurs as descrete, euhedral to subhedral grains up to 80 μm in size. Goethite is a secondary product probably after pyrite.
10 ML-575-2 quartz float disseminated by pyrite Area: Kékoro C	This polished section consists of goethite (70 %), pyrite (24 %), hematite (3 %), "electrum" (3 %) and gangue minerals. Goethite occurs as veinlets cutting quartz, and contains anhedral grains of hematite. Pyrite occurs as descrete, subhedral to euhedral grains of approximate 30 μm in size. "Electrum" sometimes occurs as isolated, anhedral grains of 40 x 20 μm in size, in small open space (about 0.2 - 0.3 mm ϕ) near the boundary between goethite veinlets and quartz.
11 M-1 quartz float Area: Kékoro	This polished section is composed of goethite (57 %), hematite (30 %), pyrite (10 %), "electrum" (3 %) and gangue minerals. Goethite shows massive, rounded and/or pseudomorphous probably after pyrite of approximate 0.1 mm in size. Hematite occurs also as psuedomorph after pyrite of about 0.2 mm in size with goethite, and as needle-like and columnar crystals up to 0.1 mm in length. Pyrite occurs as descrete, subhedral to euhedral grains of approximate 20 μm in size.
12 M-707622 silicified rock Area: Kékoro	This is composed of arsenopyrite (60 %), pyrrhotite (30 %), pyrite (10 %) and gangue minerals. Arsenopyrite occurs as aggregates of euhedral rhombic crystals up to 0.7 mm in size, and frequently contains rounded grains of pyrrhotite. Pyrrhotite occurs as aggregates of anhedral grains up to 0.2 mm in size, and was replaced into pyrite, more or less, in the later stage. Pyrite also occurs as aggregates of subhedral grains of approximate 80 x 40 μm in size, so it should be originally pyrrhotite.
13 RAZ-691700 garnet-actinolite schist Area: Baoule-Banifing	It consists of pyrrhotite (80 %), ilmenite (15 %), chalcopyrite (3 %), galena (2 %) and gangue minerals. Pyrrhotite occurs as aggregates of anhedral grains up to 0.3 x 0.1 mm in size. Subhedral grains of ilmenite up to 0.1 mm in size may be one of the primary constituents of the basaltic rock. Chalcopyrite and galena occur as anhedral grains up to 30 μm and 20 μm in size, respectively, with pyrrhotite.
14 RAZ-691950 silicified rock Area: Baoule-Banifing	It is composed of arsenopyrite (50 %), goethite (30 %), pyrite 20 %) and gangue minerals. Arsenopyrite occurs as aggregates of euhedral to subhedral crystals up to 3 x 1 mm in size. Goethite shows cubic pseudomorph probably after pyrite up to 0.6 x 0.4 mm in size. Pyrite occurs as aggregates of subhedral grains, and most of pyrite may be replacement products of pyrrhotite.
15 RMR-21912 dacite with qz veins Area: Baoule-Banifing	This polished section is composed of goethite (90 %), hematite (10 %) and gangue minerals. Goethite occurs as veinlets and networks with hematite. Hematite sometimes show cubic pseudomorph probably after pyrite.
16 DR-2 quartz vein Area: Diamou	This consists of gangue minerals and a lesser amount of pyrite. Pyrite rarely occurs as rounded, subhedral grains up to 40 μm in size in boundaries among quartz grains. Radial, elongated crystals of the gangue minerals are observed with quartz.
17 DR-12 quartz vein Area: Diamou	This polished section is composed of goethite (80 %), pyrite (20 %) and gangue minerals. Goethite occurs as aggregates of pseudomorph probably after pyrite, each cube is approximate 40 x 40 μm in size, and as those of anhedral tiny grains up to 0.2 x 0.1 mm in size. Pyrite occurs as subhedral grains up to 0.1 mm in size, and arranges like veinlets.

Apc.2 Résultat d'observation microscopique en lames polies (3/4)

18	Nag-2 silicified dacite disseminated by arsenopyrite Area: Kékoro E	This consists of arsenopyrite (50 %), pyrite (30 %), pyrrhotite (20 %) and gangue minerals. Arsenopyrite occurs as descrete, euhedral crystals of 0.3 x 0.2 mm in size. Pyrite occurs as euhedral crystals up to 0.1 mm in size and as aggregates of anhedral grains that possibly replaced pyrrhotite. Pyrrhotite occurs as aggregates of anhedral grains up to 0.2 x 0.1 mm in size.
19	Nag-3 silicified dacite disseminated by arsenopyrite Area: Kékoro E	This polished section is composed of pyrrhotite (50 %), pyrite (50 %) and gangue minerals. Pyrrhotite occurs as aggregates of anhedral grains up to 0.3 x 0.3 mm in size. Pyrite also occurs as aggregates of anhedral grains up to 0.2 x 0.2 mm in size, and includes relicts of pyrite grains.
20	R-707 silicified dacite disseminated by arsenopyrite Area: Kékoro	This polished section consists of arsenopyrite (50 %), carbonaceous matters (20 %), pyrite (20 %), pyrrhotite (10%) and gangue minerals. Arsenopyrite occurs as euhedral rhombic crystals up to 0.3 x 0.2 mm in size, and frequently contains rounded grains of pyrrhotite of approximate 30 μm in size. The carbonaceous matters occur as descrete aggegates up to 0.2 x 0.1 mm in size. Pyrite occurs as euhedral to subhedral grains that often arrange into a line like discontinuous veinlets, and also as aggregates of anhedral to subhedral grains possible replaces pyrrhotite.

Apc.2 Résultat d'observation microscopique en lames polies (4/4)

	Il	Ap	Po	Cp	Gn	Py	El	Ht	Go	CM
MAG-940-3	+		+++	++		+++			+	
MB-125						++				+++
MB-150-2						++		+	++	+++
MC-200-2	+++					+		++	+++	
MC-290						+++	(+)			
MC-320						++			+++	+++
MC-400-3							(+)			+++
MC-625-2						+++	(+)			++
MC-650-2						++				+++
ML-575-2						++	(+)	(+)	++	
M-1						++			+++	
M-707622		+++	+++			++		+++	+++	
RAZ-691700	++		+++	(+)	(+)					
RAZ-691950		+++				++			+++	
RMR-21912								++	+++	
DR-2						+++				
DR-12						++			+++	
Nag-2		+++	++			+++				
Nag-3			+++			+++				
R-707		+++	++			++			++	

Abbreviations: Il:Ilmenite, Ap:Arsenopyrite, Po:Pyrrhotite, Cp:Chalcopyrite, Gn:Galena
Py:Pyrite, El:Electrum, Ht:Hematite, Go:Goethite, CM:Carboneceous matt

+++ :abundant
++ :common
+ :little
(+) :rare

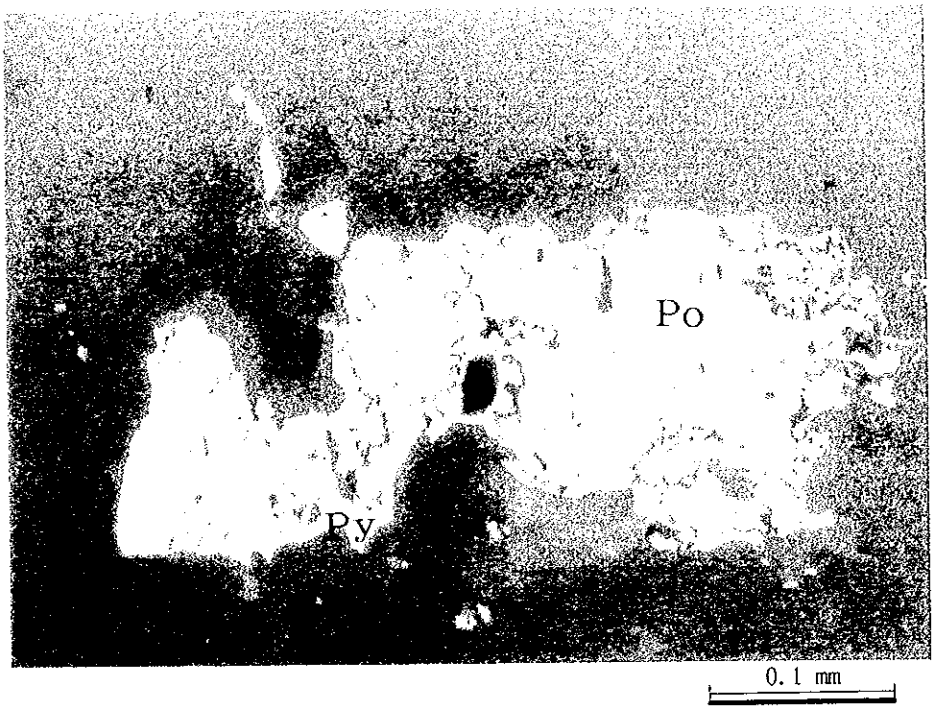

Sample No.: MAG-940-3
meta-sandstone
Location: Kekoro
Po:Pyrrhotite, Py:Pyrite

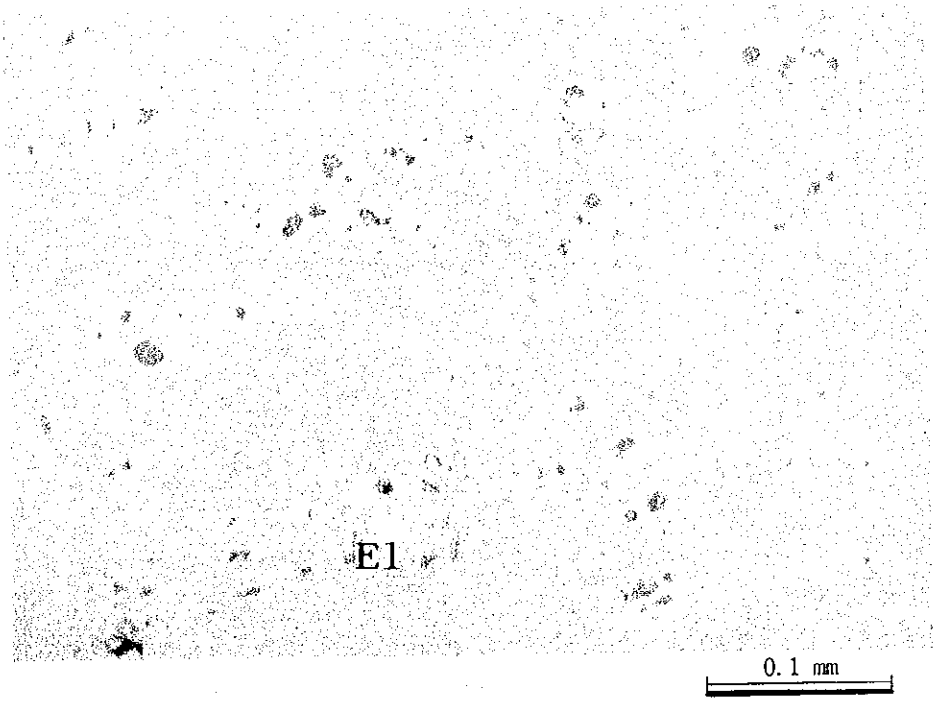

Sample No.: MC-290
quattz float
Location: Kekoro
El:Electrum

(oil)

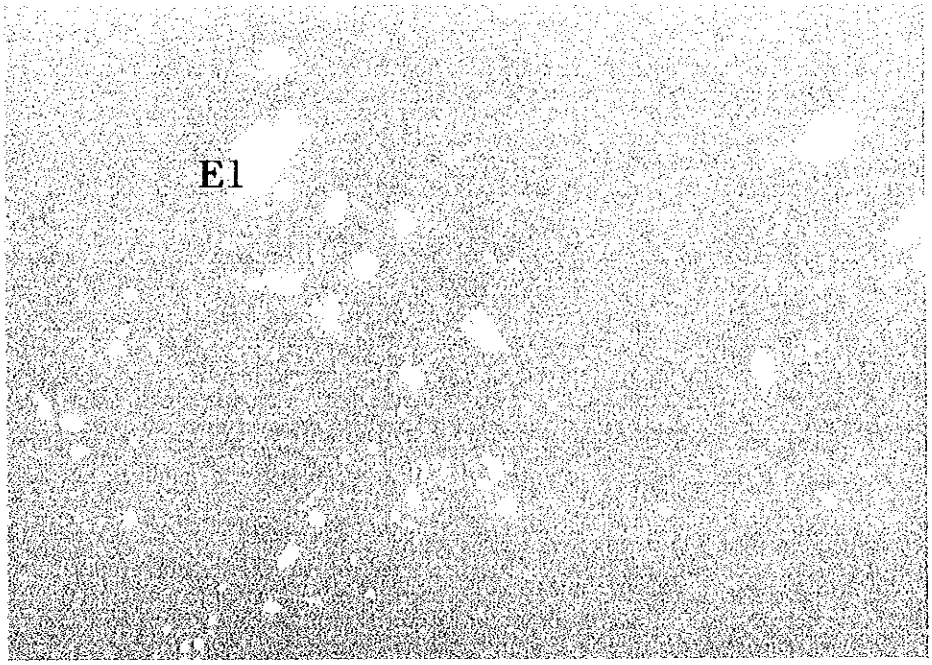

Sample No.: MC-290
quartz
Location: Kekoro
El:Electrum

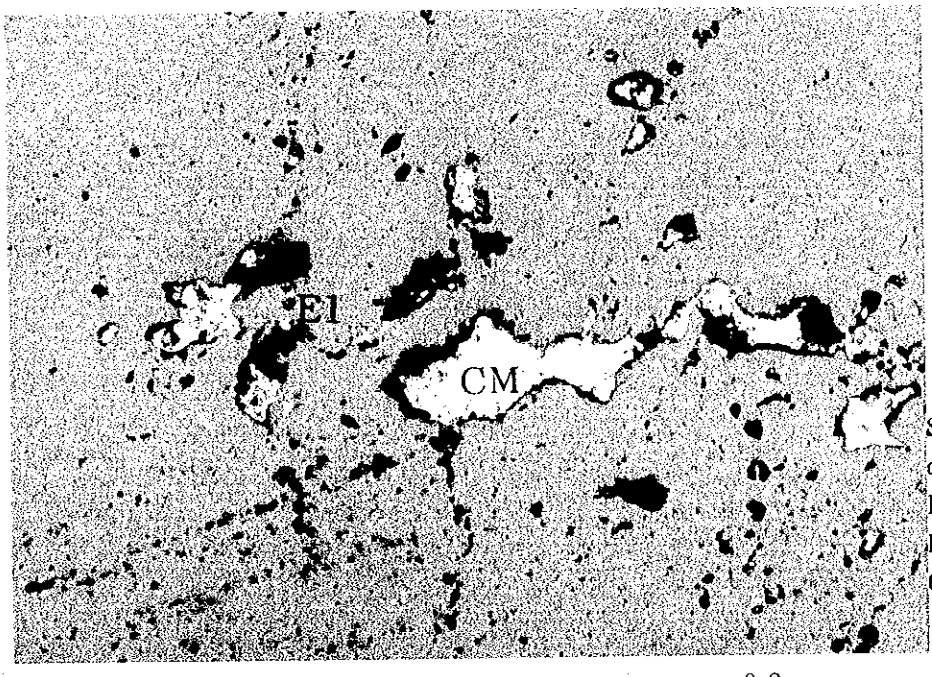

Sample No.: MC-400-3
quartz float
Location: Kekoro B
El:Electrum
CM:Carbonaceous mateers

Sample No.: ML-575-2
quartz float
Location: Kekoro D
El:Electrum

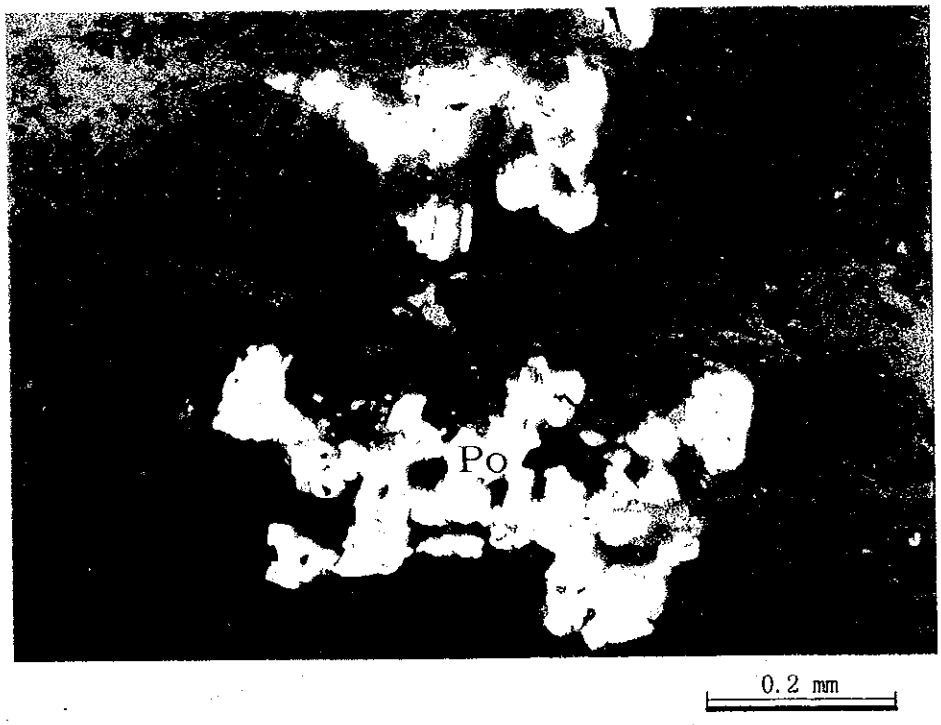

Sample No.:RAZ-691700
garnet-actinolite schist
Location: Baoule-Banifing
Po:Pyrrhotite

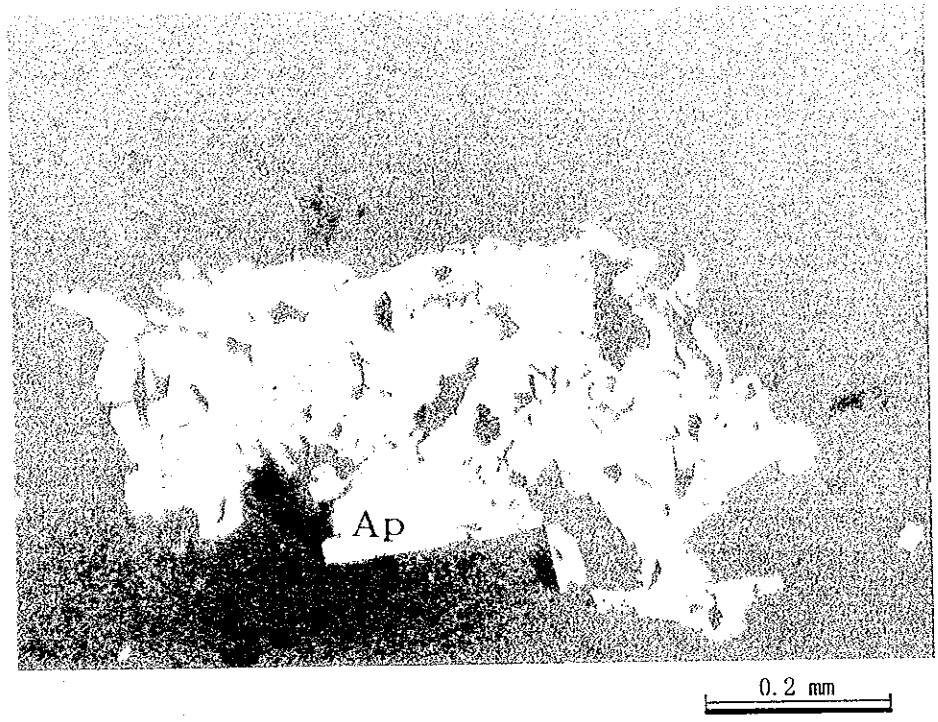

Sample No.:RAZ-691950
silicified rock
Location: Baoule-Banifing
Ap:Arsenopyrite

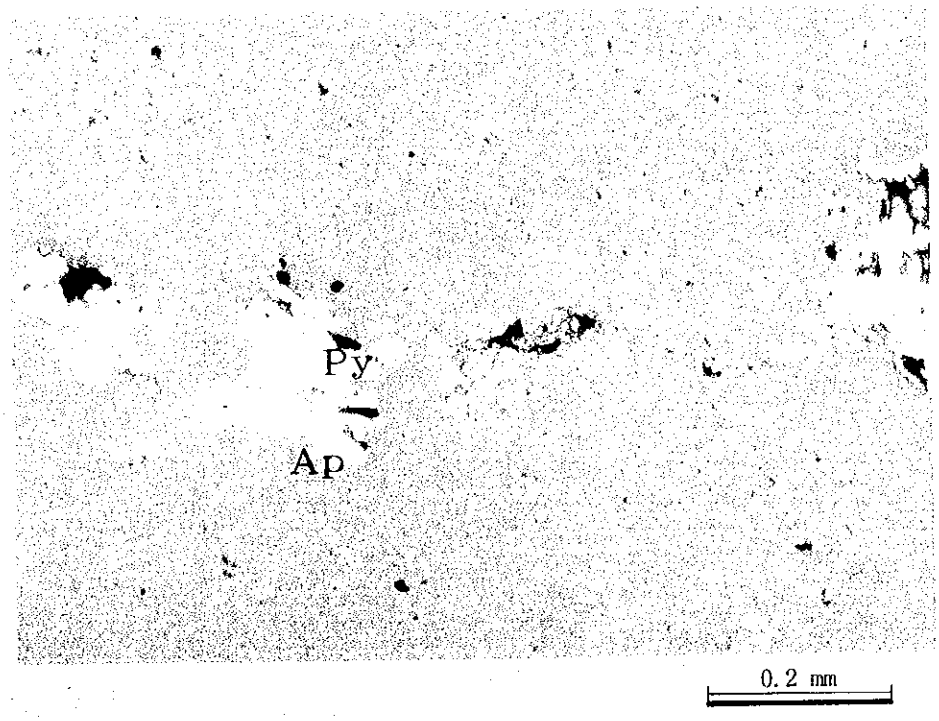

Sample No.: Nag-3
silicified dacite
Location: Kekoro
Po:Pyrrhotite, Ap:Arsenoyrite

Apc.3 Résultat de diffraction des Rayons X

Apc.3 Résultat de diffraction des Rayons X

seri. no.	sample no.	location	field name	detected minerals																
				Qz	Pl	Kf	Bi	Ser	Tm	Kao	Sm	Cal	Boe	Dia	Mt	Ht	Go	Lep	Py	Po
1	MD-150	Kékoro	quartz float	+++						(+)						(+)	(+)			(+)?
2	MM-125	Kékoro	psammitic schist	+++				+	+								+			
3	MV-175	Kékoro	silicified rhyolite	+++	+	+						+					+		+?	+
4	DS-1-4	Kékoro	laterite (pisolith), depth:4m	++						+						+	+			
5	DS-3-3	Kékoro	laterite (pisolith), depth:3m	++						+	+?			+		+?	+	+		
6	DS-3-4	Kékoro	laterite (pisolith), depth:4m	+++						+			+			+	+			
7	DS-5-1	Kékoro	laterite (pisolith), depth:1m	++						(+)		+?		+?		++	+			
8	DS-5-2	Kékoro	laterite (pisolith), depth:2m	++												+	+			
9	DS-5-4	Kékoro	laterite (pisolith), depth:4m	+++				+?		+						+	+			
10	DR-3	Diamou	altered porphyritic rock	+++	+	+		+							+?	+			+	
11	DR-6	Diamou	altered porphyritic rock	++	+	+		+								+?	+		+?	
12	RBD-714000	Baoulé-Banifing	psammitic schist	++			+	+												
13	RBF-693400	Baoulé-Banifing	fine grained meta-volcanics	++	+++	+	+	+												

+++ : abundant
++ : common
+ : little
(+) : rare

Qz: Quartz
Pl: Plagioclase
Kf: K-feldspar
Bi: Biotite
Ser: Sericite, muscovite
Tm: Turmaline(Dravite)
Kao: Kaolinite
Sm: Smectite
Cal: Calcite
Boe: Boehmite
Dia: Diaspore
Mt: Magnetite
Ht: Hematite
Go: Goethite
Lep: Lepidocrocite
Py: Pyrite
Po: pyrrohtite

Apc.4 Résultat des mesures de la température d'homogénéisation et de congélation

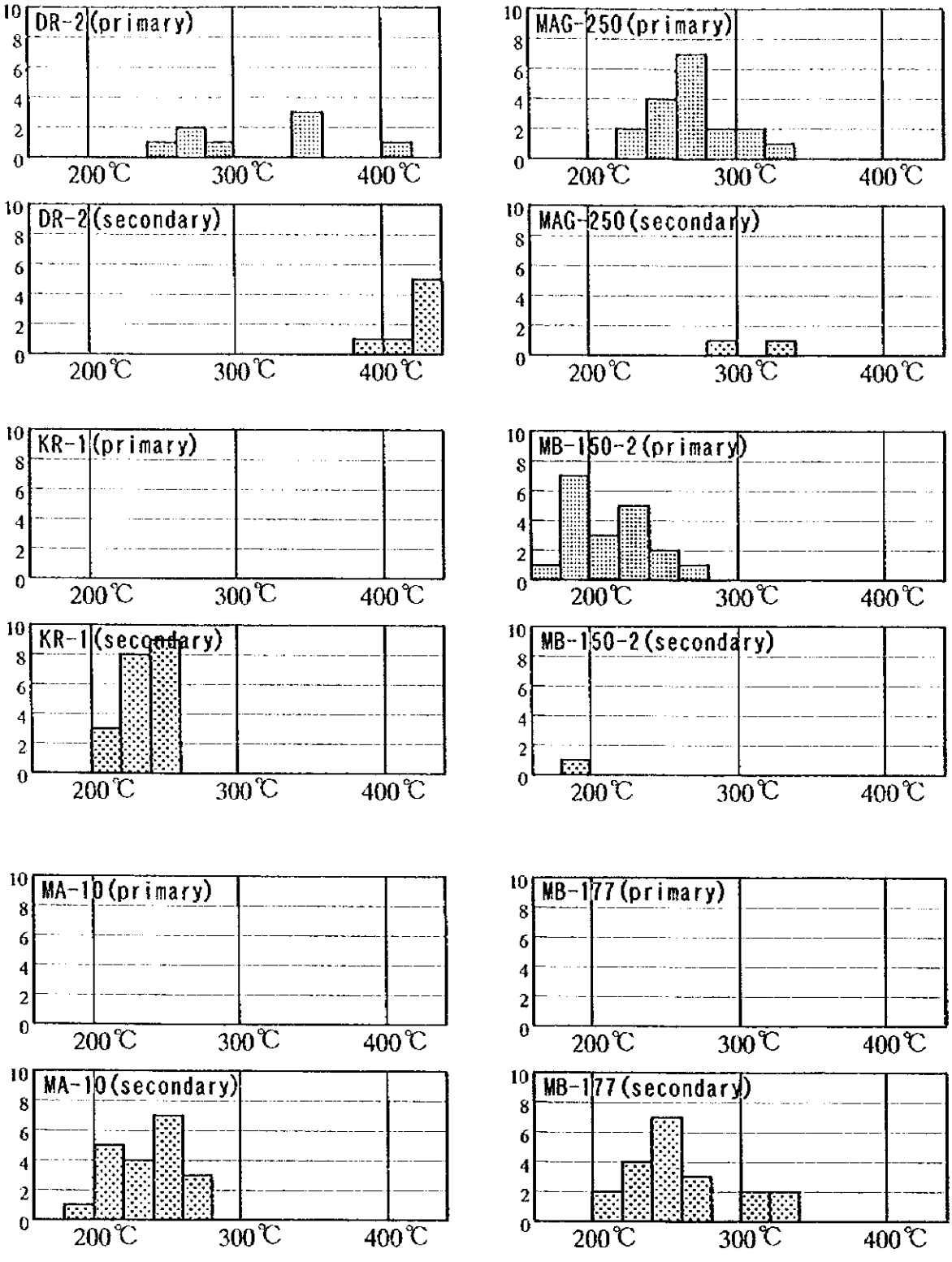

Apc.4 Résultat des mesures de la température d'homogénéisation et de congélation (1)

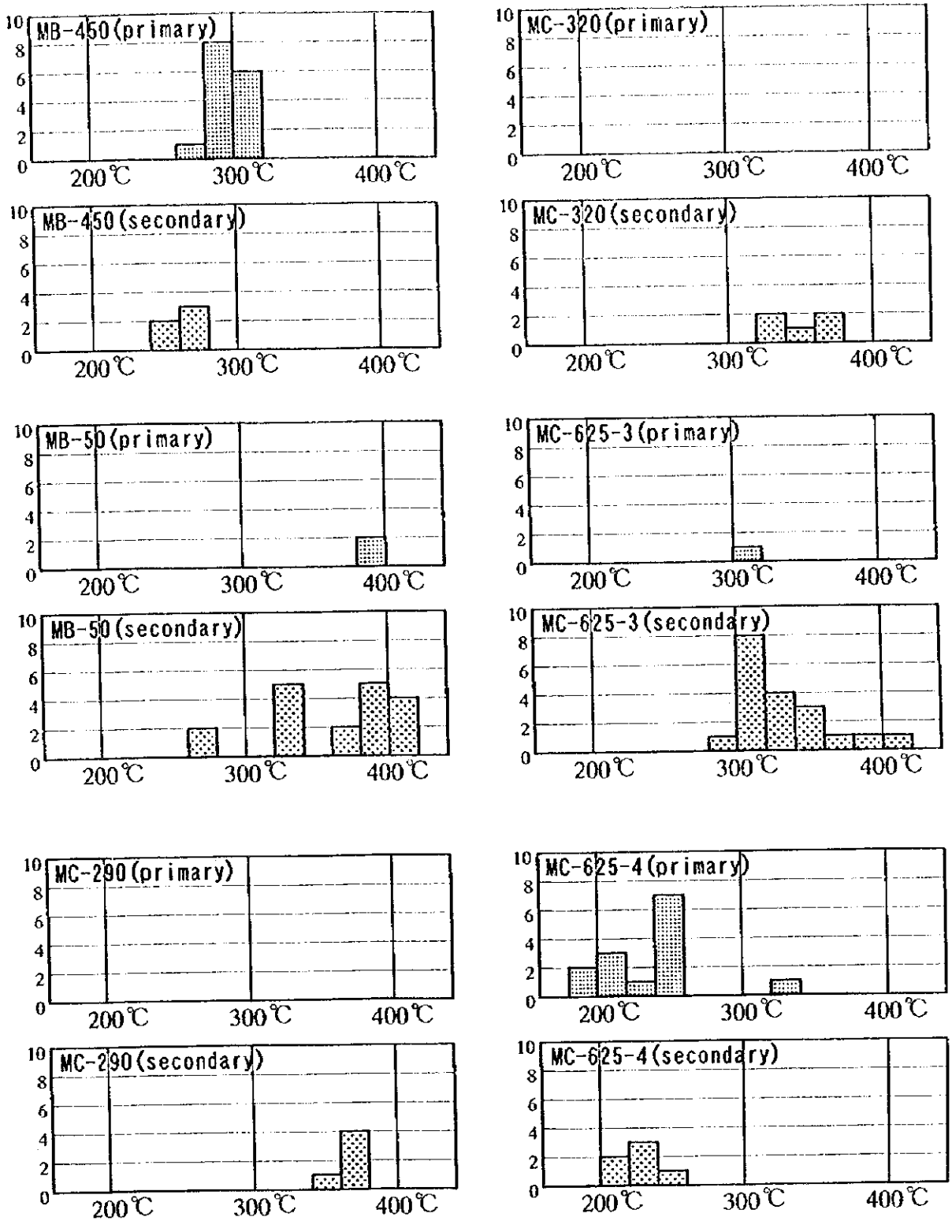

Apc.4 Résultat des mesures de la température d'homogénéisation et de congélation (2)

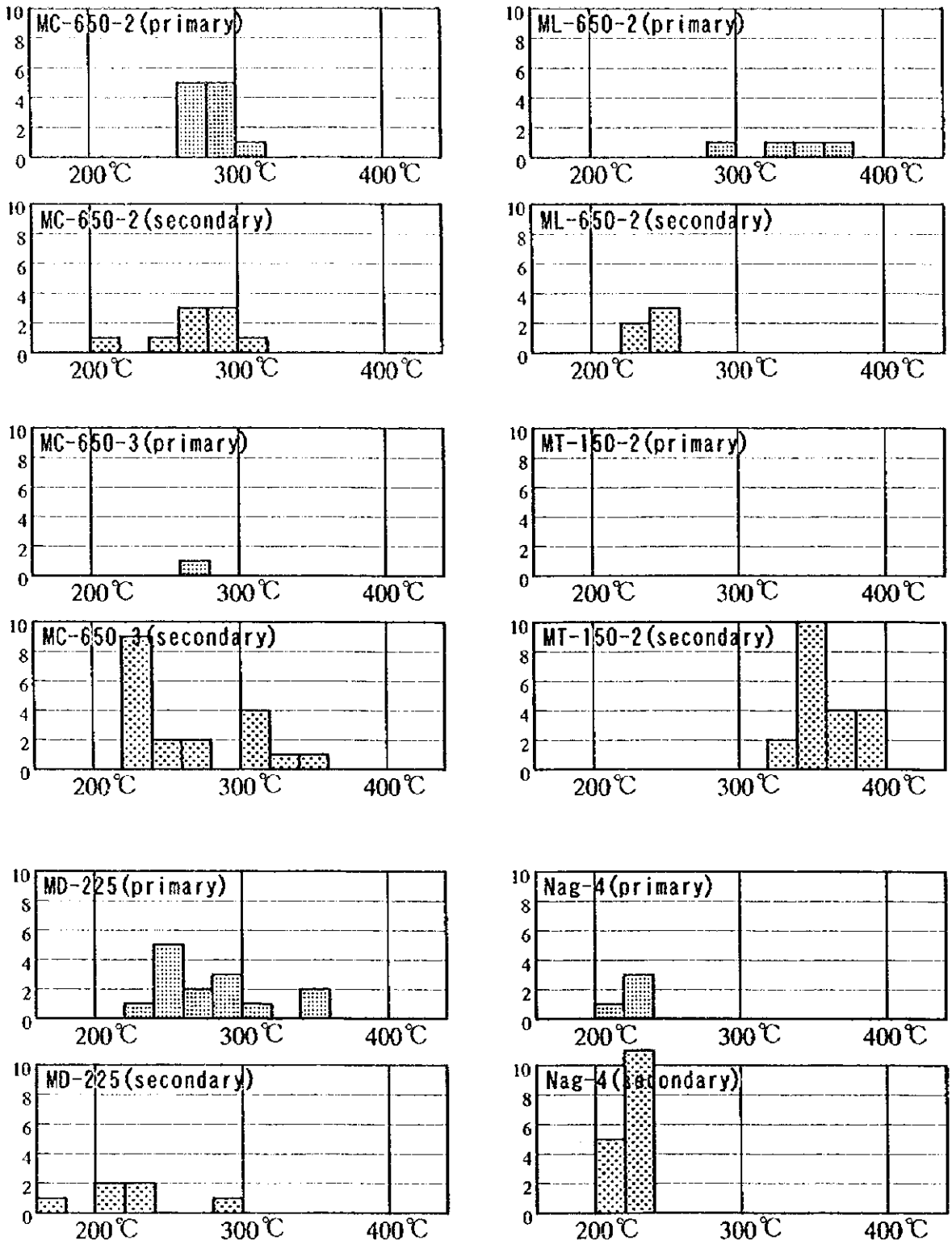

Apc.4 Résultat des mesures de la température d'homogénéisation et de congélation (3)

Apc.4 Résultat des mesures de la température d'homogénéisation et de congélation (4)

Sample		T (℃) homogenization temperature (℃)	T (℃) homogenization temperature (℃)	S (wt%) salinity (I) (equi. wt% NaCl)	Morphology	Remarks primary or secondary	Statistics	
MC-650-2	1	-	292	-	amoeba	primary	mean of T	278.5
MC-650-2	2	-	297	-	amoeba	primary	st.dev. of T	22.4
MC-650-2	3	-	295	-	elliptic	primary		
MC-650-2	4	-	300	-	elliptic	primary	mean of S	6.8
MC-650-2	5	-	286	-	circular	primary	st.dev. of S	4.9
MC-650-2	6	-	277	14.2	rectangular	primary		
MC-650-2	7	-	200	11.7	triangular	secondary		
MC-650-2	8	-	264	3.7	triangular	primary		
MC-650-2	9	-	274	3.7	square	primary		
MC-650-2	10	-	277	3.8	circular	primary		
MC-650-2	11	-	274	-	circular	primary		
MC-650-2	12	-	288	3.5	circular	primary		
MC-650-2	13	-	300	-	amoeba	secondary		
MC-650-2	14	-	273	-	elliptic	secondary		
MC-650-2	15	-	279	-	elliptic	secondary		
MC-650-2	16	-	285	-	elliptic	secondary		
MC-650-2	17	-	275	-	elliptic	secondary		
MC-650-2	18	-	286	-	circular	secondary		
MC-650-2	19	-	297	-	elliptic	secondary		
MC-650-2	20	-	251	-	circular	secondary		
MC-320	1	-	337	-	amoeba	secondary		
MC-320	2	-	340	-	amoeba	secondary		
MC-320	3	-	365	-	elliptic	secondary		
MC-320	4	-	366	-	amoeba	secondary		
MC-320	5	-	338	-	amoeba	secondary		
MB-450	1	-	282	2.7	amoeba	primary	mean of T	285.2
MB-450	2	-	292	2.6	amoeba	primary	st.dev. of T	19.7
MB-450	3	-	290	-	elliptic	primary		
MB-450	4	-	280	-	rectangular	primary	mean of S	9.2
MB-450	5	-	280	13.9	rectangular	primary	st.dev. of S	6.0
MB-450	6	-	287	-	pseudo-hexagonal	primary		
MB-450	7	-	268	-	amoeba	secondary		
MB-450	8	-	248	-	amoeba	secondary		
MB-450	9	-	249	14.0	circular	secondary		
MB-450	10	-	265	12.6	amoeba	secondary		
MB-450	11	-	262	-	amoeba	secondary		
MB-450	12	-	287	-	amoeba	primary		
MB-450	13	-	319	-	elliptic	primary		
MB-450	14	-	308	-	rectangular	primary		
MB-450	15	-	300	-	circular	primary		
MB-450	16	-	275	-	rectangular	primary		
MB-450	17	-	307	-	circular	primary		
MB-450	18	-	297	-	rectangular	primary		
MB-450	19	-	303	-	square	primary		
MB-450	20	-	305	-	rectangular	primary		
MD-225	1	-	231	3.5	rectangular	secondary	mean of T	262.2
MD-225	2	-	228	3.8	elliptic	secondary	st.dev. of T	47.7
MD-225	3	-	205	-	elliptic	secondary		
MD-225	4	-	164	3.8	rectangular	secondary	mean of S	3.6
MD-225	5	-	299	3.8	amoeba	secondary	st.dev. of S	0.2
MD-225	6	-	247	-	rectangular	primary		
MD-225	7	-	239	-	triangular	primary		
MD-225	8	-	247	3.3	rectangular	primary		
MD-225	9	-	267	-	rectangular	primary		
MD-225	10	-	249	-	elliptic	primary		
MD-225	11	-	359	-	circular	primary		

Apc.4 Résultat des mesures de la température d'homogénéisation et de congélation (5)

Sample		T (℃) homogenization temperature (℃)	T (℃) homogenization temperature (℃)	S (wt%) salinity (1) (equi. wt% NaCl)	Morphology	Remarks primary or secondary	Statistics	
MD-225	12	-	283	-	rectangular	primary		
MD-225	13	-	247	-	amoeba	primary		
MD-225	14	-	275	-	amoeba	primary		
MD-225	15	-	248	-	rectangular	primary		
MD-225	16	-	295	-	circular	primary		
MD-225	17	-	319	-	pseudo-hexagonal	primary		
MD-225	18	-	341	-	pseudo-hexagonal	primary		
MD-225	19	-	298	-	elliptic	primary		
MD-225	20	-	203	-	rectangular	secondary		
ML-650-2	1	-	233	-	pseudo-hexagonal	secondary	mean of T	281.2
ML-650-2	2	-	226	-	pseudo-hexagonal	secondary	st.dev. of T	51.2
ML-650-2	3	-	362	-	amoeba	primary		
ML-650-2	4	-	333	-	rectangular	primary		
ML-650-2	5	-	295	-	elliptic	primary		
ML-650-2	6	-	358	-	rectangular	primary		
ML-650-2	7	-	250	-	amoeba	secondary		
ML-650-2	8	-	247	-	amoeba	secondary		
ML-650-2	9	-	254	-	amoeba	secondary		
DR-2	1	-	400	-	pseudo-hexagonal	pseudo-secondary	mean of T	363.7
DR-2	2	-	428	-	elliptic	secondary	st.dev. of T	64.3
DR-2	3	-	411	-	circular	secondary		
DR-2	4	-	399	-	circular	secondary		
DR-2	5	-	421	-	circular	secondary		
DR-2	6	-	421	-	circular	secondary		
DR-2	7	-	425	-	elliptic	secondary		
DR-2	8	-	423	-	amoeba	secondary		
DR-2	9	-	267	-	3 phases (VLS)	primary		
DR-2	10	-	253	-	3 phases (VLS)	primary		
DR-2	11	-	273	-	3 phases (VLS)	primary		
DR-2	12	-	298	-	3 phases (VLS)	primary		
DR-2	13	-	347	-	3 phases (VLS)	primary		
DR-2	14	-	346	-	3 phases (VLS)	primary		
DR-2	15	-	343	-	3 phases (VLS)	primary		
MAG-250	1	276	273	6.0	negative crystal	primary	mean of T	275.2
MAG-250	2	280	278	8.4	amoeba	primary	st.dev. of T	26.6
MAG-250	3	240	238	7.3	negative crystal	primary		
MAG-250	4	282	280	6.4	amoeba	primary	mean of S	7.3
MAG-250	5	322	320	8.2	amoeba	secondary	st.dev. of S	1.1
MAG-250	6	288	286	-	amoeba	secondary		
MAG-250	7	267	265	-	negative crystal	primary		
MAG-250	8	253	251	-	negative crystal	primary		
MAG-250	9	276	274	-	amoeba	primary		
MAG-250	10	246	245	-	negative crystal	primary		
MAG-250	11	238	237	-	negative crystal	primary		
MAG-250	12	270	268	-	amoeba	primary		
MAG-250	13	278	276	-	negative crystal	primary		
MAG-250	14	260	258	-	negative crystal	primary		
MAG-250	15	307	305	-	amoeba	primary		
MAG-250	16	313	311	-	amoeba	primary		
MAG-250	17	282	280	-	amoeba	primary		
MAG-250	18	278	276	-	amoeba	primary		
MAG-250	19	337	335	-	negative crystal	primary		
MAG-250	20	248	248	-	amoeba	primary		
MB-150-2	1	204	203	-	negative crystal	primary	mean of T	210.2
MB-150-2	2	160	160	-	amoeba	primary	st.dev. of T	27.0
MB-150-2	3	201	200	-	negative crystal	primary		

Apc.4 Résultat des mesures de la température d'homogénéisation et de congélation (6)

Sample		T (℃) homogenization temperature (℃)	T (℃) homogenization temperature (℃)	S (wt%) salinity (1) (equi. wt% NaCl)	Morphology	Remarks primary or secondary	Statistics	
MB-150-2	4	191	190	-	negative crystal	secondary		
MB-150-2	5	212	211	-	negative crystal	primary		
MB-150-2	6	196	195	-	negative crystal	primary		
MB-150-2	7	200	199	-	negative crystal	primary		
MB-150-2	8	229	228	-	negative crystal	primary		
MB-150-2	9	228	227	-	amoeba	primary		
MB-150-2	10	182	182	-	amoeba	primary		
MB-150-2	11	193	192	-	negative crystal	primary		
MB-150-2	12	268	266	-	negative crystal	primary		
MB-150-2	13	227	226	-	amoeba	primary		
MB-150-2	14	239	238	-	amoeba	primary		
MB-150-2	15	247	245	-	amoeba	primary		
MB-150-2	16	235	234	-	amoeba	primary		
MB-150-2	17	196	195	-	negative crystal	primary		
MB-150-2	18	196	189	-	amoeba	primary		
MB-150-2	19	245	244	-	negative crystal	primary		
MB-150-2	20	180	180	-	amoeba	primary		
MC-625-4	1	227	225	13.5	amoeba	secondary	mean of T	233.1
MC-625-4	2	216	215	14.3	amoeba	primary	st.dev. of T	31.8
MC-625-4	3	252	250	12.8	negative crystal	primary		
MC-625-4	4	247	246	11.4	negative crystal	primary	mean of S	13.7
MC-625-4	5	228	227	16.6	amoeba	secondary	st.dev. of S	1.9
MC-625-4	6	216	215	-	amoeba	primary		
MC-625-4	7	252	250	-	amoeba	primary		
MC-625-4	8	250	248	-	amoeba	primary		
MC-625-4	9	252	250	-	amoeba	primary		
MC-625-4	10	246	245	-	negative crystal	secondary		
MC-625-4	11	244	242	-	amoeba	primary		
MC-625-4	12	230	229	-	negative crystal	primary		
MC-625-4	13	225	224	-	negative crystal	secondary		
MC-625-4	14	201	200	-	negative crystal	secondary		
MC-625-4	15	184	184	-	amoeba	primary		
MC-625-4	16	253	251	-	amoeba	primary		
MC-625-4	17	213	212	-	negative crystal	primary		
MC-625-4	18	213	212	-	amoeba	secondary		
MC-625-4	19	341	338	-	negative crystal	primary		
MC-625-4	20	200	199	-	amoeba	primary		
MA-10	1	-	209	-	triangular	secondary	mean of T	237.3
MA-10	2	-	204	-	amoeba	secondary	st.dev. of T	24.4
MA-10	3	-	207	-	hexagonal	secondary		
MA-10	4	-	206	-	hexagonal	secondary	mean of S	4.1
MA-10	5	-	203	4.3	amoeba	secondary	st.dev. of S	1.6
MA-10	6	-	199	5.8	square	secondary		
MA-10	7	-	239	-	square	secondary		
MA-10	8	-	239	-	rectangular	secondary		
MA-10	9	-	248	-	square	secondary		
MA-10	10	-	253	-	rectangular	secondary		
MA-10	11	-	268	5.5	circular	secondary		
MA-10	12	-	230	-	rectangular	secondary		
MA-10	13	-	230	-	rectangular	secondary		
MA-10	14	-	256	2.5	rectangular	secondary		
MA-10	15	-	256	-	rectangular	secondary		
MA-10	16	-	253	-	square	secondary		
MA-10	17	-	256	2.5	pseudo-hexagonal	secondary		
MA-10	18	-	266	-	circular	secondary		
MA-10	19	-	256	-	rectangular	secondary		

Apc.4 Résultat des mesures de la température d'homogénéisation et de congélation (7)

Sample		T (℃) homogenization temperature (℃)	T (℃) homogenization temperature (℃)	S (wt%) salinity (1) (equi. wt% NaCl)	Morphology	Remarks primary or secondary	Statistics	
MA-10	20	-	268	-	rectangular	secondary		
MB-177	1	-	216	0.7	circular	secondary	mean of T	257.0
MB-177	2	-	229	1.1	rectangular	secondary	st.dev. of T	33.7
MB-177	3	-	216	-	amoeba	secondary		
MB-177	4	-	247	1.2	amoeba	secondary	mean of S	0.9
MB-177	5	-	247	0.9	amoeba	secondary	st.dev. of S	0.2
MB-177	6	-	247	-	amoeba	secondary		
MB-177	7	-	248	-	amoeba	secondary		
MB-177	8	-	278	0.7	triangular	secondary		
MB-177	9	-	260	-	rectangular	secondary		
MB-177	10	-	222	-	triangular	secondary		
MB-177	11	-	231	-	amoeba	secondary		
MB-177	12	-	234	-	rectangular	secondary		
MB-177	13	-	240	-	rectangular	secondary		
MB-177	14	-	304	-	rectangular	secondary		
MB-177	15	-	324	-	triangular	secondary		
MB-177	16	-	306	-	hexagonal	secondary		
MB-177	17	-	321	-	amoeba	secondary		
MB-177	18	-	250	-	triangular	secondary		
MB-177	19	-	278	-	rectangular	secondary		
MB-177	20	-	242	-	rectangular	secondary		
MC-650-3	1	-	271	3.3	square	primary	mean of T	265.3
MC-650-3	2	-	330	3.5	rectangular	secondary	st.dev. of T	36.9
MC-650-3	3	-	230	-	triangular	secondary		
MC-650-3	4	-	230	-	rectangular	secondary	mean of S	3.5
MC-650-3	5	-	232	-	rectangular	secondary	st.dev. of S	0.2
MC-650-3	6	-	232	-	rectangular	secondary		
MC-650-3	7	-	278	3.5	rectangular	secondary		
MC-650-3	8	-	238	-	square	secondary		
MC-650-3	9	-	231	-	amoeba	secondary		
MC-650-3	10	-	237	-	hexagonal	secondary		
MC-650-3	11	-	236	-	amoeba	secondary		
MC-650-3	12	-	340	3.7	square	secondary		
MC-650-3	13	-	305	3.7	amoeba	secondary		
MC-650-3	14	-	279	-	rectangular	secondary		
MC-650-3	15	-	245	-	rectangular	secondary		
MC-650-3	16	-	250	-	rectangular	secondary		
MC-650-3	17	-	233	-	circular	secondary		
MC-650-3	18	-	307	-	rectangular	secondary		
MC-650-3	19	-	301	-	rectangular	secondary		
MC-650-3	20	-	300	-	rectangular	secondary		
Nag-4	1	-	223	8.6	square	primary	mean of T	219.9
Nag-4	2	-	223	7.5	triangular	primary	st.dev. of T	6.0
Nag-4	3	-	223	6.4	circular	primary		
Nag-4	4	-	221	-	rectangular	secondary	mean of S	7.2
Nag-4	5	-	222	-	rectangular	secondary	st.dev. of S	1.1
Nag-4	6	-	225	-	rectangular	secondary		
Nag-4	7	-	227	-	square	secondary		
Nag-4	8	-	220	-	hexagonal	secondary		
Nag-4	9	-	221	-	hexagonal	secondary		
Nag-4	10	-	220	-	hexagonal	secondary		
Nag-4	11	-	217	-	square	secondary		
Nag-4	12	-	219	-	square	secondary		
Nag-4	13	-	222	-	square	secondary		
Nag-4	14	-	213	-	square	secondary		
Nag-4	15	-	210	-	rectangular	secondary		

Apc.4 Résultat des mesures de la température d'homogénéisation et de congélation (8)

Sample		T (℃) homogenization temperature (℃)	T (℃) homogenization temperature (℃)	S (wt%) salinity (1) (equi. wt% NaCl)	Morphology	Remarks primary or secondary	Statistics	
Nag-4	16	-	208	5.8	rectangular	primary		
Nag-4	17	-	208	-	rectangular	secondary		
Nag-4	18	-	220	7.7	rectangular	secondary		
Nag-4	19	-	225	-	rectangular	secondary		
Nag-4	20	-	230	-	rectangular	secondary		
KR-1	1	-	212	6.5	rectangular	secondary	mean of T	234.5
KR-1	2	-	215	-	hexagonal	secondary	st.dev. of T	13.2
KR-1	3	-	207	-	rectangular	secondary		
KR-1	4	-	220	-	rectangular	secondary	mean of S	4.4
KR-1	5	-	229	-	amoeba	secondary	st.dev. of S	1.8
KR-1	6	-	229	2.1	rectangular	secondary		
KR-1	7	-	240	-	rectangular	secondary		
KR-1	8	-	247	-	rectangular	secondary		
KR-1	9	-	248	-	amoeba	secondary		
KR-1	10	-	254	5.1	rectangular	secondary		
KR-1	11	-	232	-	rectangular	secondary		
KR-1	12	-	250	-	amoeba	secondary		
KR-1	13	-	243	-	amoeba	secondary		
KR-1	14	-	231	3.0	rectangular	secondary		
KR-1	15	-	230	5.2	circular	secondary		
KR-1	16	-	247	-	rectangular	secondary		
KR-1	17	-	243	-	amoeba	secondary		
KR-1	18	-	232	-	rectangular	secondary		
KR-1	19	-	239	-	rectangular	secondary		
KR-1	20	-	241	-	circular	secondary		
MB-50	1	-	278	2.9	rectangular	secondary	mean of T	362.9
MB-50	2	-	279	-	amoeba	secondary	st.dev. of T	41.5
MB-50	3	-	323	-	circular	secondary		
MB-50	4	-	323	-	circular	secondary	mean of S	2.0
MB-50	5	-	325	-	circular	secondary	st.dev. of S	0.6
MB-50	6	-	330	-	triangular	secondary		
MB-50	7	-	330	1.2	rectangular	secondary		
MB-50	8	-	376	-	amoeba	secondary		
MB-50	9	-	382	-	hexagonal	primary		
MB-50	10	-	382	-	rectangular	secondary		
MB-50	11	-	382	-	circular	secondary		
MB-50	12	-	382	-	circular	secondary		
MB-50	13	-	393	2.2	square	primary		
MB-50	14	-	404	-	rectangular	secondary		
MB-50	15	-	404	1.9	square	secondary		
MB-50	16	-	407	1.7	square	secondary		
MB-50	17	-	417	-	triangular	secondary		
MB-50	18	-	383	-	rectangular	secondary		
MB-50	19	-	380	-	circular	secondary		
MB-50	20	-	377	-	circular	secondary		
MC-625-3	1	-	341	1.8	hexagonal	secondary	mean of T	328.3
MC-625-3	2	-	300	2.8	amoeba	secondary	st.dev. of T	30.8
MC-625-3	3	-	313	2.2	square	secondary		
MC-625-3	4	-	319	1.8	rectangular	secondary	mean of S	3.2
MC-625-3	5	-	308	7.3	elliptic	primary	st.dev. of S	2.4
MC-625-3	6	-	344	-	amoeba	secondary		
MC-625-3	7	-	337	-	square	secondary		
MC-625-3	8	-	301	-	rectangular	secondary		
MC-625-3	9	-	325	-	rectangular	secondary		
MC-625-3	10	-	322	-	square	secondary		
MC-625-3	11	-	294	-	square	secondary		

Apc.4 Résultat des mesures de la température d'homogénéisation et de congélation (9)

Sample		T (℃) homogenization temperature (℃)	T (℃) homogenization temperature (℃)	S (wt%) salinity (1) (equi. wt% NaCl)	Morphology	Remarks primary or secondary	Statistics	
MC-625-3	12	-	309	-	square	secondary		
MC-625-3	13	-	325	-	square	secondary		
MC-625-3	14	-	311	-	elliptic	secondary		
MC-625-3	15	-	301	-	square	secondary		
MC-625-3	16	-	364	-	rectangular	secondary		
MC-625-3	17	-	349	-	elliptic	secondary		
MC-625-3	18	-	387	-	rectangular	secondary		
MC-625-3	19	-	304	-	triangular	secondary		
MC-625-3	20	-	411	-	square	secondary		
MC-290	1	-	364	-	triangular	secondary	mean of T	363.0
MC-290	2	-	370	-	amoeba	secondary	st.dev. of T	7.6
MC-290	3	-	351	-	hexagonal	secondary		
MC-290	4	-	369	-	amoeba	secondary		
MC-290	5	-	361	-	square	secondary		
MT-150-2	1	-	393	-	square	secondary	mean of T	361.9
MT-150-2	2	-	392	10.6	square	secondary	st.dev. of T	19.8
MT-150-2	3	-	376	-	amoeba	secondary		
MT-150-2	4	-	382	10.7	circular	secondary	mean of S	10.7
MT-150-2	5	-	396	-	square	secondary	st.dev. of S	0.1
MT-150-2	6	-	349	-	square	secondary		
MT-150-2	7	-	352	-	circular	secondary		
MT-150-2	8	-	345	-	circular	secondary		
MT-150-2	9	-	339	-	amoeba	secondary		
MT-150-2	10	-	348	-	amoeba	secondary		
MT-150-2	11	-	359	-	elliptic	secondary		
MT-150-2	12	-	346	-	rectangular	secondary		
MT-150-2	13	-	350	-	triangular	secondary		
MT-150-2	14	-	335	-	square	secondary		
MT-150-2	15	-	342	-	square	secondary		
MT-150-2	16	-	347	-	triangular	secondary		
MT-150-2	17	-	355	-	square	secondary		
MT-150-2	18	-	377	-	triangular	secondary		
MT-150-2	19	-	378	-	hexagonal	secondary		
MT-150-2	20	-	377	-	square	secondary		